Flora xxx (xxxx) xxx–xxx

Contents lists available at ScienceDirect

Flora

journal homepage: www.elsevier.com/locate/flora

Plant functional indicators of vegetation response to climate change, past present and future: II. Modal plant functional types as response indicators for present and future climates☆

Andrew N. Gillison

Center for Biodiversity Management, P.O. Box 120, Yungaburra, Queensland, 4884, Australia

ARTICLE INFO

Edited by: Hermann Heilmeier

Keywords:
Plant–climate indicators
Modal PFTs
Bioclimate
Species distribution modeling
Green stem photosynthesis
Leaf inclination
Leaf stomatal distribution

ABSTRACT

An assessment of plant functional indicators of vegetation response to climate change requires a science-based evaluation of functional linkages between plants and climate. This paper addresses the hypotheses outlined in the preceding paper: 1) A whole-plant system of modal plant functional types (PFTs) based on a core set of functional traits can provide an improved alternative to PFTs and traits used so far in models of vegetation response to climate change; 2) Modal PFTs are more efficient indicators of vegetation response to climate change than individual traits; 3) Improved plant functional selection criteria can lead to improved parameters in Earth System and Dynamic Global Vegetation Models. Present-day (1975 centred) plant–climate relationships were analyzed within a global climatic framework of 1327 (200 m^2) sample sites covering all major biomes. Five regions were selected for their range of bioclimatic gradients (arctic-boreal; cool temperate-subtropical; humid equatorial; hot, cold deserts). Biophysical site data were recorded along gradient oriented transects (gradsects) using a standard protocol that included all vascular plant taxa and modal PFTs. Regression, ordination and species distribution modeling were used to assess plant–climate indicator values against ten bioclimatic variables including extremes of contemporary thermal, light (energy) and moisture availability and estimates for 'present' (1975) and year 2100 climate scenarios. Modal PFTs and individual traits were highly correlated in differing patterns with bioclimate in each of the five regions in both climate scenarios with PFTs being the best predictors. Each of the three hypotheses is supported by these results, indicating that preference should be given to modal assemblages rather than individual traits as response parameters in predictive vegetation models. The indicators identified here are but one element of the highly complex array of other factors that influence vegetation response to terrestrial environmental change such as resource use, species acclimation, invasive species and human population pressure.

1. Introduction

Global concern surrounding the impact of climate change is reflected in the increasing frequency of models that seek to predict vegetation response under future climate scenarios. Inevitably, the extent of their success will be governed primarily by the quality and accuracy of the underlying data. The preceding paper (Gillison, this volume) showed that, to a large extent, model parameters that rely on plant functional traits are constrained by a high level of inconsistency in trait selection and measurement. In most studies there is a prevailing focus on the use of individual plant functional traits rather than their coordinated functional performance at whole-plant level. Recent experimental and empirical evidence now suggests however, that, instead of relying solely on single functional traits (FTs), an evaluation of whole-plant function or 'fitness' is required to assess vegetation performance under contemporary climates and for predicting outcomes under climate change. In the preceding paper an overview of case studies involving the use of individual FTs and whole-plant modal plant functional types (PFTs) in both paleovegetation reconstruction and present day vegetation revealed an array of widely differing methods that highlight the need for consistency and uniformity in trait selection, measurement and analysis. That overview identified key issues that led to the following hypotheses: 1) A whole-plant system of modal plant functional types (PFTs) based on a core set of functional traits can provide an improved alternative to PFTs and traits used so far in models of vegetation response to climate change; 2) Modal PFTs are more

☆ This article is part of a special issue entitled: "Functional traits explaining plant responses to past and future climate changes" published at the journal Flora 254C, 2019.

E-mail address: andygillison@gmail.com.

https://doi.org/10.1016/j.flora.2019.04.001

0367-2530/ © 2019 Elsevier GmbH. All rights reserved.

efficient indicators of vegetation response to climate change than individual traits; 3) Improved plant functional selection criteria can lead to improved parameterization in Earth System and Dynamic Global Vegetation Models. The aim of this paper is to address these three hypotheses by evaluating trait performance at multiple scales using both individual functional traits and their assemblages as a whole-plant modal PFT.

The idea of a 'whole-plant' syndrome of interacting and integrated functional traits expressed as a 'modal PFT' is a relatively novel concept. For this reason, the remainder of this section that is mostly derived from the preceding paper, outlines the conceptual development of plant functional traits and their whole-plant assemblages as plant functional types (PFTs) (Gillison, 2013). Unfortunately, pervasive lack of consensus among ecologists worldwide restricts a common working definition of PFTs and functional traits. Following Albert et al. (2010) with reference to fitness, as defined by Gillison (2013), PFTs are '*any measureable plant trait combinations with potential to influence whole-plant fitness*' applied here specifically to whole-plant assemblages of individual functional traits or analogous plant functional elements (PFEs), (Gillison, 2002, 2013).

An initial holistic approach to a 'whole-plant' assemblage of 'plant functional attributes' (Gillison (1981) was paralleled by the structural-functional types of Box (1981, 1996) and other functional typologies (Keddy, 1992; Gillison and Carpenter, 1997; Lavorel et al., 1997, 1999, 2007; Díaz et al., 2002) that centered around an assumption that specific trait assemblages represented a measure of plant 'fitness' that involved capacity to adapt to environmental change. As applied in this paper and as indicated by Schulze (1982) 'fitness' is considered at whole plant level e.g. where carbon allocation strategies are accounted for in terms of photosynthesis, biomechanical support, transport, nutrient and water acquisition as well as regeneration and reproduction. In this context, individual trait influence on fitness will be a function of its integration and coordination with other functional traits within a plant individual. It is now widely assumed that overall fitness can be achieved through adaptive strategies that ensure a net benefit between increased gains in carbon assimilation and the costs of resource acquisition. Theories underlying such strategies are well described, for example, the Leaf–Height–Seed (LHS) strategy of Westoby (1998) and the more encompassing Leaf Economic Spectrum (LES) of Wright et al. (2004) and Díaz et al. (2016) including the much earlier CSR (Competitors–Stress–Ruderal) strategy (Grime, 1977; Pierce et al., 2017). The Leaf–Life form–Root (LLR) strategy described by Gillison (2013) complements the CSR, LHS and LES systems by the inclusion of additional significant photosynthetic traits such as leaf inclination (Myneni et al., 1986; Falster and Westoby, 2003; Wang et al., 2007; Lapola et al., 2008; Posada et al., 2009; Mason et al., 2012a), leaf phyllotaxis or insertion pattern such as rosettes (Withrow, 1932; Lavorel et al., 1998, 1999; Diaz et al. (2007); Bernhardt-Römermann et al., 2011) and green-stem photosynthesis (Nedoff et al., 1985; Gibson, 1996; Gregory, 1996; Pfanz, 1999; Yiotis et al., 2008; Bloemen et al., 2016; Liu et al., 2018). These traits constitute important plant adaptations to irradiance, nutrition and water availability and are considered here as key functional elements in the construction of whole-plant functional models.

Unlike most systems that infer global trends in plant functional performance using specific trait subsets, LLR also includes functional traits of succulent vegetation that occurs mainly in environmental extremes with high moisture deficits and forms a highly significant proportion of world flora (ca.10,000 species; Oldfield, 1997). In the LLR system specific trait syndromes or PFTs are termed plant functional *modi* (Gillison, 1981) representing whole-plant functional modality (*cf*. Violle et al., 2007). Functional *modi* described hereafter as *modal PFTs*, are constructed using an assembly-rule set and syntactical grammar based on 36 generic plant functional elements (PFEs)

Table 1
Plant functional traits and elements (PFEs) used in this study.

Functional trait	Element code	Description	
[*Photosynthetic envelope*]			
Leaf size	nc	no repeating leaf units	
	pi	picophyll	$< 2mm^2$
	le	leptophyll	2 – 25
	na	nanophyll	25 – 225
	mi	microphyll	225 – 2025
	no	notophyll	2025 – 4500
	me	mesophyll	4500 – 18200
	pl	platyphyll	18200 – 36400
	ma	macrophyll	$36400 – 18 \times 10^4$
	mg	megaphyll	$> 18 \times 10^4$
Leaf inclination	ve	vertical	>30° above horizontal
	la	lateral	±30° to horizontal
	pe	pendulous	>30° below horizontal
	co	composite	
Leaf chlorotype	do	dorsiventral	
	is	isobilateral or isocentric	
	de	Deciduous	(Perennials)
	ct	cortic	(photosynthetic stem)
	ac	achlorophyllous	(without chlorophyll)
Leaf morphotype	ro	rosulate or rosette	
	so	solid 3-D	
	su	succulent	
	pv	parallel-veined	
	fi	filicoid (fern)	(Pteridophytes)
	ca	carnivorous	(e.g. *Nepenthes*)
[*Supporting vascular structure*]			
Life form	ph	phanerophyte	
	ch	chamaephyte	
	hc	hemicryptophyte	
	cr	cryptophyte	
	th	therophyte	
	li	liana	
Root type	ad	adventitious	
	ae	aerating	(e.g. pneumatophore)
	ep	epiphytic	
	hy	hydrophytic	
	pa	parasitic	

(Gillison and Carpenter, 1997; Gillison, 2002) (Table 1, SI Table 2) (SI Fig. 3, in the preceding paper). The system comprises a many-to-many mapping whereby more than one modal PFT can be represented within a species and vice versa. A typical modal PFT for an individual of *Acer palmatum* for example, might be a mesophyll (*me*) leaf size class with pendulous (*pe*) inclination, dorsiventral (*do*) (hypostomatous), deciduous (*de*) leaves with green-stem (cortex) (*ct*) photosynthesis supported by a phanerophyte (*ph*), the resulting modal PFT combination being coded as *me-pe-do-de-ct-ph*. Change in any one element of the modal construct for the same species, such as an increase in leaf size (e.g. mesophyll to notophyll) along a moisture gradient, results in a new *modus* (*no-pe-do-de-ct-ph*). The method is thus sensitive to phenotypic and intraspecific variation under changing environments and is thus relevant to detecting and potentially forecasting vegetation response to climate change. The methodology is described in detail elsewhere (Gillison, 2002, 2013) and can be readily applied in practice using the VegClass software package (Gillison, 2002).

2. Materials and methods

2.1. Selection of plant functional traits and types

The pervasive lack of consensus in the selection and application of a universal set of functional types (FTs) for application worldwide

ARTICLE IN PRESS

indicates that: a) The emergence of a global patchwork of uncoordinated datasets of varying quality limits their application in predictive modeling of vegetation response to environmental change across temporal and spatial scales. b) Most FTs in current use require laboratory support that restricts their application in many field-based operations. c) Varying consistency in laboratory procedures continues to raise concerns about the validity of their application in comparative studies. This paper aims to avoid these deficiencies through the selection of plant functional variables according to the following criteria:

a) A parsimonious set of FTs should be selected that represents core elements of plant functional strategies of resource acquisition and conservation with application worldwide.
b) FTs should be readily observable and repeatable by different observers in the field and reduce the need for laboratory support. Quantitative measures of field based FTs should complement detailed ecophysiological measurement and analysis of plant function.
c) Whole-plant integrated sets of FTs require a consistent and logical means of PFT assembly that underpins strategies of resource acquisition and conservation across multiple scales.
d) The construction of a global database of whole-plant PFTs requires a uniform recording and field data sampling protocol that is amenable to numerical analysis across multiple scales.

Following these criteria, a global database was compiled according to a standard data recording procedure for site physical attributes and vegetation structure (SI Tables 1 and 2). Modal PFTs were constructed from 36 generic FTs (here termed plant functional elements or PFEs) according to a prescribed assembly rule set (Gillison and Carpenter, 1997), Table 1 (SI Table 2) (SI Fig. 3, in the preceding paper). The database structure compiled using VegClass (Gillison, 2002) facilitates comparative numerical analysis across multiple scales (Gillison, 2002, 2013). Previous investigations using this technology have demonstrated the predictive capacity of modal PFTs as bioindicators at local and bioregional scales (Jones et al., 2003; Bardgett, 2005; Gillison et al., 2013), supporting their consideration as potential indicators of biodiversity response to environmental change.

2.2. Site selection and sampling

Study sites were positioned along gradient directed transects 'gradsects' following the principle that the distribution of living organisms is governed primarily by environmental gradients rather than by random or stochastic events (Gillison and Brewer, 1985; Gillison et al., 2016; Gillison, 2018) (see also Ludwig and Cornelius, 1987; Wessels et al., 1998; Brohman and Bryant, 2005; Parker et al., 2011; Ferrer-Paris et al., 2013; Wrubel and Parker, 2018). Gradsects provide a logistically efficient sample design where the aim is to record species distribution and identify environmental drivers of that distribution. For this reason it has become widely applied by many research institutions (FAO, Wong et al., 2001; The World Bank, Gillison et al., 2016; USDA 2005; USA NPS, 2012; National Geographic Society, Bimeda, 2018). Compared to traditional statistical requirements that demand random sampling under often logistically demanding randomised site locations, the underlying statistical model for gradsect methodology allows for purposive site location along known environmental gradients. Apart from logistic efficiency, the method has several advantages, namely that it is known to enhance the likelihood of locating rarities and improve environmental representativeness and thereby species distribution modeling. Data for the present study were extracted from a current database with 1327 (40 m × 5 m) (200 m^2) plots within a series of regional gradsects across latitudes and elevations representing more than 90% of global climate variation based on key elements of temperature, precipitation and evapotranspiration (Fig. 1). As part of the site selection process, similarity mapping of global climate was undertaken with the (public domain) DOMAIN package (Carpenter et al., 1993), one of many species distribution modeling (SDM) programs in common use (Elith and Franklin, 2013; Franklin et al., 2015), (see also Booth et al., 1987, 2014). DOMAIN has an advantage in that it runs efficiently on a limited number of field records of taxa or PFTs that is often the case in field surveys.

Within the global climate framework, five regional gradsect clusters were selected according to key climate and other biophysical gradients ranging from alpine tundra and hot and cold deserts, to humid equatorial rain forests and landscape mosaics of multiple vegetation types including primary and secondary forest, agroforest plantations, pastures, crops, volcanic heath, maritime dune sequences and freshwater and intertidal swamps. In this respect, the site location and predictive modeling in this treatment are designed to accommodate 'disturbance' response rather than a fixed or steady-state equilibrium model that implies no temporal or spatial vegetation response to disturbance ('disturbance' defined here as measureable loss of taxa or live tissue). Regional gradsects were selected to represent environmental gradients that embrace wide-ranging response patterns to environmental change including disturbance. As the modal PFTs used in this study are sensitive to such change they are well suited as a tool for monitoring vegetation and biodiversity response to climate change including human-induced physical disturbance (Gillison et al., 2013). In addition to climate-driven filters (thermal, light (energy), moisture), each regional gradsect includes disturbance filters that also influence vegetation response to factors such as fire, wind and water as well as grazing, periodic or episodic herbivory, invasive organisms and human-induced habitat loss. The positioning of sample sites along regional gradients in this way allows for the establishment of wide-ranging ecological reference points that enhance the detection of response to environmental change between gradient extremes and for subsequent geophysical relocation and and re-arrangement of floristic and PFT composition under climate change. Because such re-arrangement will also be subject to uncontrolled forecasting of mainly human-induced modification and other related stochastic events, the predictive modeling of vegetation response described here must be considered within that overall context.

As indicated in Fig. 1, the first of these gradsects was located in the Russian Far East (RFE) that included the Kamchatka peninsula (Kamchatsky krai) and a mainland area near Vladivostok (Primorsky krai) (33 sites). The second region was located in the Eastern Himalaya (Bhutan) (48 sites) with the third in Indomalesia, including the Indonesian islands of Sumatra and Java (46 sites). Regions 4 and 5 included a 'cold' continental desert in the Gobi region of Outer Mongolia (35 sites) and a 'hot' desert in the Namib (24 sites) respectively (site detail in SI Annexes A, B, C, D, E). The data for all sites (SI Tables 1,2) were recorded by the author, using a standard proforma, in most cases with team assistance and institutional support through national herbaria where available. Where possible, in each locality, plant voucher specimens were collected for subsequent identification. Unlike most vegetation recording methods at this global scale that tend to focus on specific vegetation sub-groups, all vascular plant taxa as well as corresponding modal PFTs were recorded in each 200 m^2 plot enabling a more comprehensive assessment of community composition and analysis than is usually the case in broad-ranging vegetation surveys.

2.3. Data acquisition and management using the VegClass system

Field data were compiled using the VegClass software (Gillison, 2002) that provides metadata summaries and analytical output that can be exported using industry standard formats such as Excel. A numerical functional 'distance' matrix between modal PFTs can be generated in

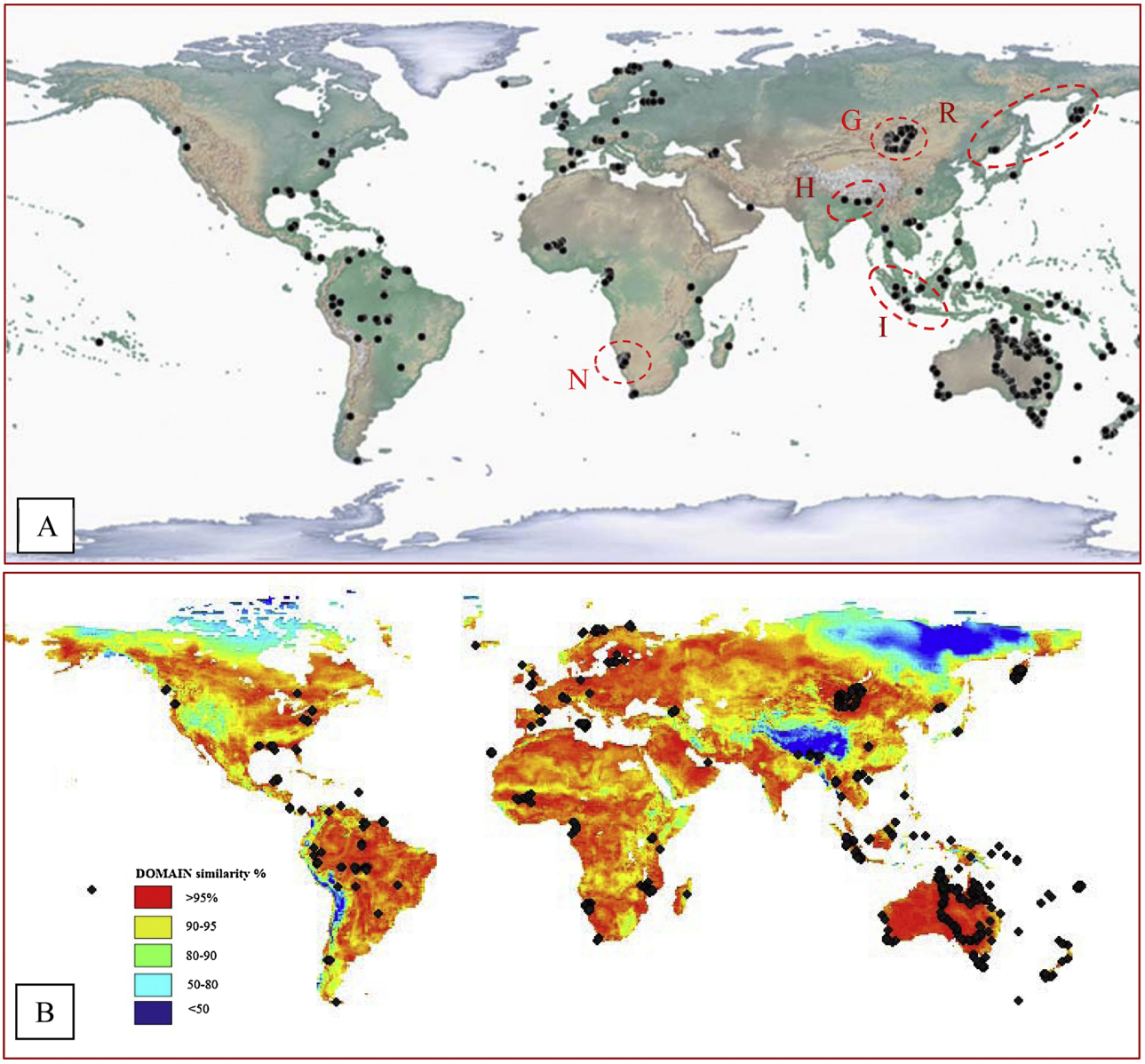

Fig. 1. Distribution of 1327 sample locations (black dots) used in this study (A). Five selected regional sample areas are (R) Russian Far East, (G) Gobi cold desert, Mongolia, (H) Eastern Himalaya (Bhutan, Nepal), (I) Indomalesia (Sumatra, Java), (N) Namib hot desert, (Namibia). Lower figure (B) shows Domain similarity map of global climate coverage based on minimum temperature of the coldest week (°C) mean annual precipitation (mm yr^{-1}), annual actual evapotranspiration (mm), and elevation (m).

VegClass and was used in comparing and analysing plant assemblages at multiple scales. The global data set compiled using a standard recording proforma covering all major latitudes and climates that support plant growth (Gillison, 2018), indicates that, based on this study, a global approximation of unique modal PFTs is 3,500 or about one percent of the world's approximately 350,000 vascular plant species. Apart from functional diversity measures (not used here), a separate measure of plant functional complexity (PFC) (Gillison, 2002), based on a minimum-spanning-tree distance of PFT values within a transect (Gillison and Carpenter, 1997), provided a simple means of inter-site comparisons for example, where the number of PFTs in different sites may be the same or similar, but where their modal complexity differs. The PFC measure for each site is thus not a 'diversity index' (*sensu* Magurran, 1988) but approximates the Rao quadratic entropy coefficient that is widely applied as a measure of functional diversity (Mason et al., 2012b; Carmona et al., 2015; Vandewalle et al., 2014; Zhang et al., 2015; de Bello et al., 2016; Fontana et al., 2016). As such, PFC has been found useful as a bioindicator within and between continents (Gillison, 2012; Gillison et al., 2013). Being independent of species, PFC is a useful complementary measure to modal PFTs, especially where species identification can be problematic as in poorly documented vegetation in widespread areas of the humid tropics, remote mountain sites or extensive karst regions.

ARTICLE IN PRESS

Table 2
Bioclim variables used in this study.*

Variable number	Variable	Minimum temp (°C)	Maximum temp (°C)	Rainfall (mm mth^{-1})	Radiation (W m^{-2} d^{-1})	Pan Evap. (mm d^{-1})
Bio03	Isothermality (Bio2-Bio07)	x	x			
Bio04	Temperature seasonality (CV)	x	x			
Bio05	Max temperature warmest week (°C)		x			
Bio06	Min temperature of coldest week (°C)	x				
Bio12	Annual precipitation (mm yr^{-1})			x		
Bio15	Precipitation seasonality (CV)					
Bio23	Radiation seasonality (CV)					
Bio26	Radiation of warmest quarter (W m^{-2})	x	x		x	x
Bio31	Moisture index seasonality (CV)			x		
Bio33	Mean moisture index of driest quarter			x		x

* See complete list of 36 Bioclim variable codes through CliMond (Kriticos et al., 2012).

2.4. Climate data

Climate data were obtained using the Bioclim register in CliMond (Kriticos et al., 2012, 2014). The CliMond archive is a set of free climate data products, modeling tools, and the home of the Bioclim registry. The climate data includes interpolated surfaces at 10′ and 30′ for recent historical climate and relevant future climate scenarios, available as monthly climate data, with 40 Bioclim variables (https://www.climond.org/). The Bioclim system is extensively used in modeling the distribution of living organisms with respect to bioclimate (Booth et al., 1987, 2014; Busby, 1991) and is thus relevant to the present treatment. As indicated in the foregoing, effective distribution models require access to the range of environmental extremes occupied by the taxa and PFTs under study (*cf.* Schimper, 1903). Although a wide range of elevational extremes (0–4600 m) was recorded in this study, elevation is not regarded as a primary climate variable as it reflects compounded effects of topography (aspect) and thermal and precipitation regimes that, in turn, are influenced by factors such as variation in regional adiabatic lapse rates and continentality including the so-called Massenerhebung effect common in maritime zones. While elevation is thus excluded from the data analyses, for descriptive purposes it is included in SI Annexes, A, B, C, D, E. In order to facilitate numerical analysis of vegetation and bioclimate relationships across the environmental extremes represented in the five regional gradsects, ten Bioclim variables (Table 2) were selected from the CliMond register using data estimated for the CM101975HV1.2, and CM102100A1BCSBioV1.2 scenarios (centred on years 1975 and 2100 respectively). The geocoded data from CliMond were converted into gridded ASCII format compatible with DOMAIN. Additional elevation data not accessible directly in CliMond were kindly made available by D. Kriticos (pers. comm.). In order to assess potential trends in vegetation response to climate change, for comparative analysis, the CliMond data set for *'present climate'* 1961–1990 (30 years centred on 1975) was matched against predicted bioclimate for the year 2100 *'future climate'*. A detailed discussion of the rationale underlying the selection of both climate scenarios is available elsewhere (Kriticos et al., 2012, 2014; IPCC Climate Change, 2007). Significantly, no comparable climate data were available for a numerical analysis of paleovegetation and paleoclimate. For each region separately, the relative individual contribution of each Bioclim variable to regional bioclimate was assessed by regressing each variable against ordination scores (two axes) of all Bioclim variables (SI Table 3). As a result of this procedure, two Bioclim variables Bio03 Isothermality and Bio04 temperature seasonality (CV) were excluded from subsequent analyses due to resulting low predictive coefficients overall.

2.5. Data compilation and analyses

Data acquired from 1327 (40 m × 5 m) (200 m^2) plots included 36,207 records of 25,637 vascular plant taxa and 3403 species-weighted (number of species with the attribute) unique modal PFT trait combinations or syndromes. The large size of the overall data set mitigates against its inclusion in the Supplementary section. Instead, original data and metadata summaries can be accessed through an international digital data repository (https://dataDryad.org/) using the following link doi: 10.5061/dryad.jj946rq. For the reasons outlined in the foregoing, the present paper focuses primarily on the information value that can be acquired from the analysis of modal PFTs. In cases where statistical analysis may be restricted by relatively low counts of each unique PFT per transect, significant supplementary information can often be acquired through the disaggregation of PFTs into their component PFEs often resulting in higher counts per PFE per transect than their parent modal PFTs. (In the present global analysis 3403 modal PFTs generated 185,094 PFE counts). Here the statistical advantages of PFE analysis are also reflected in the reduced number of generic PFEs (in the present case 36) compared to the often much larger number of unique modal PFTs worldwide. While PFE correlates with environmental variables can provide informative general response trends in certain traits, (e.g. deciduousness, cortical photosynthesis), ultimately, results from any PFE-based analysis must be considered within the context of the functional role of each PFE within its parent modal PFT. In this study the relative values of both PFTs and PFEs as indicators of climate change are presented region by region.

Evidence for predictive relationships between the plant data and bioclimate was analysed first using the complete global data set and then each region separately. Non-linearity is a common feature in such data composites. Linear and quadratic (Pearson) regression was undertaken for all sites using Minitab version 16.2.4 and SigmaPlot 12.5. For each regional gradsect, all 8 Bioclim variables were regressed against the plant-based data (plot counts of PFTs and PFEs (plant functional elements as individual traits), species, PFT richness and PFC) in a search for potential climate indicators (Table 3). As an example of indicator potential, the response of modal PFTs and PFEs with highest correlation values to mean annual precipitation (MAP) under the two climate change scenarios, is summarised in Tables 4 and 5.

A more direct example of quantification of plant functional response to actual change is the difference in MAP between the two climate scenarios (year 2100 minus year 1975) providing a measure of change within and between regional sites (Tables 6 and 7) with PFTs and PFEs selected according to the highest correlates. Many ecological studies of FTs rely on community mean values of traits that run the risk of masking significant fine scale phenotypic and intraspecific response to changeable environmental filters. To a large degree this is avoided in the present study, as trait–environment response is quantified on a one-to-one basis using modal PFTs that are generally sensitive to such fine scale (e.g. phenotypic or intraspecific) response patterns. Depending on the level of analysis, modal PFT and PFE data can be scaled to a specific purpose and scale (e.g. plot to biome). Issues remain, nonetheless, as to

ARTICLE IN PRESS

Table 3
Correlations between species and, modal PFT richness and Plant Functional Complexity (PFC) and bioclimate across five global regions.*

Region`		Present climate (based on 1975 scenario)			Year 2100		
	Bioclim variable	Species	PFT	PFC	Species	PFT	PFC
Russian	MTWWK	–	–	0.427	–	–	0.443
Far East				0.013 (15.6)			0.010 (15.6)
(arctic- boreal)	MTCWK	–	–	–	–	–	–
	ANPRC	–	–	−0.405	–	–	−0.489
				0.019 (13.7)			0.004 (21.4)
	CVAPR	0.433	0.498	0.626	0.485	0.548	0.653
		0.12 (16.1)	0.003 (22.4)	0.001 (37.3)	0.004 (21.0)	0.001 (27.8)	0.001 (40.8)
	RWQ	–	0.356	0.505	0.371	0.412	0.555
			0.042 (9.9)	0.003 (23.1)	0.033 (11.0)	0.017 (14.3)	0.001 (28.5)
	MICV	0.423	0.446	0.558	0.441	0.476	0.591
		0.014 (15.3)	0.009 (17.3)	0.001 (28.9)	0.010 (16.8)	0.005 (20.1)	0.001 (32.8)
	MMIDQ	−0.381	−0.415	−0.552	−0.396	−0.436	−0.576
		0.029 (11.7)	0.016 (14.5)	0.001 (28.2)	0.023 (12.9)	0.011 (16.4)	0.001 (31.0)
Bhutan	MTWWK	–	–	–	–	–	–
E. Himalaya	MTCWK	–	–	–	–	–	–
(cool temp., sub-tropical)	ANPRC	–	–	–	–	–	–
	CVAPR	–	0.313		0.313	–	–
			0.030 (7.8)		0.030 (7.8)		
	RWQ	–	–	–	–	–	–
	MICV	–	0.305	–	0.305	–	–
			0.035 (7.3)		0.035 (7.3)		
	MMIDQ	–	–	–	–	–	–
Indonesia	MTWWK	–	−0.367	−0.390	–	−0.328	−0.367
			0.012 (11.5)	0.007 (13.4)		0.026 (8.7)	0.012 (13.3)
(Sumatra, Java)	MTCWK	–	−0.376	−0.394	–	−0.373	−0.414
			0.010 (12.2)	0.007 (13.6)		0.011 (11.9)	0.005 (14.5)
(humid equatorial)	ANPRC	–	–	–	0.339	–	0.292
					0.021 (9.50)		0.049 (6.5)
	CVAPR	−0.334	–	–	−0.536	–	–
		0.023 (9.1)			0.001 (27.1)		
	RWQ	–	–	–	–	–	–
	MICV	−0.373	–	–	−0.475	–	–
		0.11 (11.9)			0.001 (20.8)		
	MMIDQ	–	–	–	0.445	–	–
					0.002 (18.0)		
Mongolia	MTWWK	−0.493	−0.389	0.536	−0.547	−0.451	0.521
		0.003 (24.3)	0.021 (12.6)	0.001 (26.6)	0.001 (27.8)	0.007 (17.9)	0.001 (24.9)
Gobi cold desert	MTCWK	–	–	–	–	–	–
	ANPRC	0.729	0.710	–	0.711	−0.687	–
		0.001 (51.8)	0.001 (48.9)		0.001 (49.0)	0.001 (45.6)	
	CVAPR	0.574	−0.528	0.382	−0.651	0.588	0.473
		0.001 (30.9)	0.001 (25.7)	0.024 (12.0)	0.001 (40.7)	0.001 (32.6)	0.004 (20.0)
	RWQ	−0.361	0.383	–	–	–	–
		0.033 (10.4)	0.023 (12.1)				
	MICV	0.562	0.561	–	–	–	–
		0.001 (29.5)	0.001 (29.3)				
	MMIDQ	0.681	0.632	−0.391	0.697	0.644	−0.410
		0.001 (44.8)	0.001 (38.1)	0.020 (12.7)	0.001 (47.0)	0.001 (39.7)	0.014 (14.3)
Namibia	MTWWK	–	–	–	–	–	–
Namib hot desert	MTCWK	−0.510	–	–	−0.450	–	–
		0.011 (22.6)			0.027 (16.6)		
	ANPRC	0.854	0.812	0.590	0.860	0.871	0.653
		0.001 (71.6)	0.001 (64.3)	0.002 (31.9)	0.001 (72.8)	0.001 (74.8)	0.001 (40.0)
	CVAPR	–	–	–	–	–	–
	RWQ	–	–	–	0.502	–	–
					0.012 (8.2)		
	MICV	0.722	0.584	0.439	0.761	0.653	0.512
		0.001 (52.2)	0.003 (31.1)	0.032 (15.6)	0.001 (56.0)	0.001 (40.1)	0.011 (22.9)
	MMIDQ	–	–	–	–	–	–

* MTWWK (Maximum temperature of warmest week, °C), MTCWK (Minimum temperature of the coldest week, °C), ANPRC (Annual precipitation, mm yr^{-1}), CVAPR (Annual precipitation seasonality CV), RWQ (Radiation of the warmest quarter, W m^{-2}), MICV (Moisture Index seasonality CV), MMIDQ (Mean moisture index of the driest quarter). Cell upper r value, cell lower P value, (r^2 adj.%). Only correlates with $P < 0.05$ listed. (See Sect. 2.3 for PFC estimation method).

which scales are most appropriate for predictive models of plant functional response to climate change. Exploratory data analysis (PATN v.3) (Belbin, 1992) was used to seek evidence for corresponding pattern between the plant data and bioclimate. Two-dimensional ordination axis values were obtained from a Gower metric association measure where multi-dimensional scaling (MDS) was applied using the semi-strong-hybrid (SSH) scaling option in PATN to avoid potential bias common in alternative metric and non-metric scaling procedures. The resulting ordination values of PFTs and individual PFE counts per plot were then regressed against those of the bioclimate ordinations as a means of detecting corresponding matches with bioclimate (SI Table 4).

To explore likely patterns of vegetation response to climate change

ARTICLE IN PRESS

Table 4
Regional response of modal PFTs listed alphabetically and with highest correlation values to mean annual precipitation (MAP) under the two climate change scenarios (1975–2100).*

Region	Present climate			Year 2100	
	Response (Modal PFT)	*r* / *P*	r^2 (adj) %	*r* / *P*	r^2 (adj)%
Russian Far East	no-la-do-de-ch	−0.608	46.2	−0.756	66.0
		0.001		0.001	
(arctic-boreal)	me-la-do-de-ct-ph	−0.625	37.1	−0.733	52.2
		0.001		0.001	
	mi-la-do-de-ct-ph	−0.254	3.4	−0.370	10.9
		0.153		0.034	
	no-la-do-de-ct-ph	−0.570	30.3	−0.736	52.7
		0.001		0.001	
	le-ve-do-de-hc	0.625	37.1	0.605	34.6
		0.001		0.001	
Bhutan	me-la-do-ch	0.684	45.6	0.684	45.6
		0.001		0.001	
(cool temperate– sub-tropical)	no-la-do-ch	0.437	17.4	0.436	17.3
		0.002		0.002	
	na-la-do-fi-hc-ad	0.430	16.7	0.428	16.6
		0.002		0.002	
	le-la-do-de-fi-hc-ad	−0.424	16.2	−0.425	16.2
		0.003		0.003	
	mi-la-do-hc-ad	0.408	14.8	0.407	14.8
		0.004		0.004	
	na-la-do-de-hc-ad	−0.400	14.2	−0.400	14.2
		0.005		0.005	
	na-la-do-de-cr	−0.396	13.6	−0.396	13.8
		0.005		0.005	
Indonesia	pl-la-do-ct-ph	0.246	n.s.	0.592	33.6
		0.100		0.001	
(humid equatorial)	me-la-do-ct-ph	0.062	n.s.	0.465	19.8
		0.682		0.001	
	me-la-do-ph-li	−0.086	n.s.	0.318	8.1
		0.571		0.031	
	no-la-do-ph-li	−0.026	n.s.	0.300	6.9
		0.863		0.043	
Mongolia	na-ve-do-th	0.578	31.4	0.595	33.4
		0.001		0.001	
(Gobi cold desert)	na-ve-do-de-cr	0.481	20.8	0.476	20.3
		0.003		0.004	
	na-ve-do-de-hc	0.464	19.1	0.475	20.2
		0.005		0.004	
	na-ve-do-de-pv-hc	0.466	19.3	0.465	19.3
		0.005		0.005	
	na-la-do-th	0.436	16.6	0.418	14.9
		0.009		0.013	
	mi-ve-do-th	0.429	16.0	0.431	16.1
		0.010		0.010	
Namibia	mi-ve-do-ch	0.672	42.7	0.782	59.3
		0.001		0.001	
(Namib hot desert)	na-ve-do-ch	0.545	26.5	0.514	23.1
		0.006		0.010	

* For coding of modal PFTs see Table 1 for plant functional elements (PFEs).

at global scale, the global bioclimate datasets based on 'present climate' (the 1975 compilation) and estimates for the year 2100 were classified to 20 groups for each climate scenario separately using a PATN Gower association metric from which mean values for each constituent Bioclim variable were extracted for each group member (SI Tables 5 and 6) and a two-dimensional MDS performed on these mean values. Clusters from the graphed ordinates for the 20 group members using a minimum spanning tree were then examined subjectively for corresponding pattern of vegetation type trajectories for present and future climate. For the global data set and for each regional gradsect, DOMAIN similarity mapping was undertaken using the same bioclimatic variables estimated via the CliMond registry for both climate scenarios. Within the resulting DOMAIN map, for each of the five regions, each gradsect site cluster was then manually framed to contain the smallest rectangular pixel space and the included pixel values range-standardized using the available option in DOMAIN. The resulting values were then mapped relative to the original DOMAIN similarity map to provide a more sensitive visual appraisal of changing pattern for both present and future climate. In a separate exercise, total global field counts of modal PFTs and PFEs were sorted in descending value in order to assess their relative contribution to the world's flora as indicated by the data records from this study.

3. Results

Results are presented first, region by region and then in regional and global summaries. Due to the complex and very extensive data set with high *N* values (global and regional), regression analyses generated a very large number of statistically significant correlations, a great many with $P < 0.001$, between modal PFTs and PFEs and most bioclimate variables but especially involving moisture availability (soil moisture index and MAP). Because of the large number of samples and relatively

ARTICLE IN PRESS

Table 5
Regional response of Plant Functional Elements (PFEs) with highest correlation values to mean annual precipitation (MAP) under the two climate change scenarios (1975–2100).*

Region	Present climate			Year 2100	
	Response PFE	*r* / *P*	r^2 (adj) %	*r* / *P*	r^2 (adj)%
Russian Far East	Phanerophyte (ph)	−0.692	46.2	−0.819	66.0
		0.001		0.001	
(Arctic-boreal)	Notophyll (no)	−0.693	46.3	−0.815	65.4
		0.001		0.001	
	Cortical p/s (ct)	−0.650	40.4	−0.781	59.7
		0.001		0.001	
Bhutan	Deciduous (de)	−0.794	62.3	−0.793	62.1
		0.001		0.001	
(Temperate-subtropical)	Liana (li)	0.662	42.6	0.661	42.5
		0.001		0.001	
	Nanophyll (na)	−0.637	39.3	−0.636	39.2
		0.001		0.001	
	Mesophyll (me)	0.607	35.5	0.607	35.5
		0.001		0.001	
	Epiphytic (ep)	0.591	33.5	0.589	33.3
		0.001		0.001	
	Cryptophyte (cr)	−0.570	31.0	−0.569	30.9
		0.001		0.001	
Indonesia	Leptophyll (le)	0.540	27.6	0.368	11.6
		0.001		0.012	
(Humid equatorial)	Mesophyll (me)	−0.077	n.s.	0.341	9.6
		0.611		0.020	
	Platyphyll (pl)	0.111	n.s.	0.518	25.1
		0.461		0.001	
	Vertical incl. (ve)	0.473	20.6	0.209	n.s.
		0.001		0.163	
	Cortical p/s (ct)	−0.050	n.s.	0.317	8.0
		0.753		0.032	
Mongolia	Nanophyll (na)	0.813	65.0	0.794	61.9
		0.001		0.001	
(Gobi cold desert)	Dorsiventral (do)	0.782	59.9	0.763	56.9
		0.001		0.001	
	Cryptophyte (cr)	0.657	41.5	0.635	38.6
		0.001		0.001	
	Therophyte (th)	0.629	37.7	0.635	37.7
		0.001		0.001	
	Rosette (ro)	0.559	29.2	0.530	25.9
		0.001		0.001	
	Isobilateral (is)	−0.546	27.7	−0.541	27.1
		0.001		0.001	
	Solidiform (so)	−0.528	25.7	−0.519	24.7
		0.001		0.001	
Namibia	Dorsiventral (do)	0.883	76.9	0.914	82.7
		0.001		0.001	
(Namib hot desert)	Hemicryptophyte (hc)	0.885	77.3	0.882	76.7
		0.001		0.001	
	Microphyll (mi)	0.806	63.3	0.888	77.9
		0.001		0.001	
	Vertical incl. (ve)	0.816	65.1	0.841	69.4
		0.001		0.001	
	Parallel veined (pv)	0.706	47.5	0.715	48.9
		0.001		0.001	
	Chamaephyte (ch)	0.695	46.0	0.735	52.0
		0.001		0.001	

* For coding of modal PFTs see Table 1 for plant functional elements (PFEs).

few predictors, a correction such as OPA for Pearson *r* values was not considered necessary (Humphreys et al., 2019). For these reasons and for presentation purposes, only those variables from each data set were selected that represented the most statistically and ecologically meaningful correlates between bioclimate variables and plant-based variables (PFTs, PFEs, PFC) as well as diversity (richness) counts for species and PFTs. The following regional descriptions include species names and their modal PFE combination (e.g. *Potentilla fruticosa*, le-co-do-dech) (see Table 1 for PFE code). To conserve presentation space, the number of species names with connections to their modal PFTs is kept to a minimum in the text. The following examples (Fig. 2) of displacement patterns in PFEs and a leading (most frequent) modal PFT that can be estimated under climate change, are given in parentheses for the Russian Far East, the E. Himalaya (Bhutan) and Indonesia. For presentation purposes, both the Gobi and Namib deserts are excluded in this graphical presentation where, instead, the displacement patterns for these desert regions are tabulated in detail below (3.4, 3.5). Section 3.6 summarises the key findings of the regional and global analyses.

3.1. Russian Far East (RFE)

Differing patterns in the relationship between functional traits, PFTs and climate reflect vegetation structure and composition, ranging from alpine tundra to tall lowland broadleaf and conifer forest and coastal

ARTICLE IN PRESS

Table 6
Regional modal PFT response to differences in mean annual precipitation under the two climate change scenarios (1975–2100) listed alphabetically and according to highest correlation values.*

Region	Modal PFT	*r* (adj. r^2 %)
R.F.E.	na-ve-do-de-hc	0.556 (28.7)
	pi-ve-do-de-hc	0.549 (27.9)
	mi-ve-do-de-hc	0.528 (25.6)
	na-ve-do-de-pv-hc	0.495 (22.1)
	no-la-do-de-ch	−0.806 (63.8)
	no-la-do-de-ct-ph	−0.810 (64.6)
	me-la-do-de-ch-li	−0.742 (54.5)
	me-la-do-de-ct-ph	−0.737 (52.9)
	no-la-do-de-ph	−0.691 (46.1)
	na-co-do-pv-ph	−0.654 (40.9)
	me-la-do-de-ph	−0.622 (36.7)
	me-la-do-de-ch	−0.645 (39.7)
	mi-co-do-pv-hc-ad	−0.609 (35.1)
	le-la-do-ro-fi-hc	−0.594 (33.2)
Bhutan	me-la-do-ch	−0.687 (46.0)
	no-la-do-ch	−0.444 (18.0)
	na-la-do-fi-hc-ad	−0.443 (17.1)
	mi-la-do-hc-ad	−0.416 (15.5)
	na-la-do-de-hc-ad	0.399 (14.1)
	na-la-do-de-cr	0.399 (14.1)
	le-la-do-de-fi-hc	0.422 (16.0)
Indonesia	me-la-do-ct-ph	0.513 (24.5)
	me-la-do-ph-li	0.502 (23.5)
	pl-la-do-ct-ph	0.443 (17.8)
	no-la-do-ct-ph	0.433 (16.9)
	me-la-do-ph	0.418 (15.6)
	no-la-do-ph-li	0.415 (15.3)
Gobi desert	–	–
Namib desert	mi-ve-do-pv-hc	−0.774 (58.1)
	mi-ve-do-hc	−0.719 (49.4)
	mi-co-do-pv-hc	−0.655 (40.3)
	na-ve-do-ch	−0.551 (27.2)

* Pearson *r* values show direction of correlation with adj. r^2 % in parenthesis. All $P < 0.005$.

dune ecosystems that exist along very pronounced thermal and moisture gradients. In the present case, most significant correlates are with moisture (mean moisture index during the driest quarter, mean annual precipitation (MAP), temperature (minimum temperature of the coldest month) and radiation (CV and warmest quarter)). At high elevations in alpine tundra (≈1100 −1500 m), species typified by small, vertically inclined leaves such as *Loiseleuria procumbens, Oxytropis pumilio* (le-ve-do-de-hc) are highly and positively correlated with MAP under both climate scenarios (Table 4) which is the reverse for woody taxa and PFTs at lower elevations (≈5–500 m) (SI Annex A) with larger, laterally inclined leaves and green stem (cortical) photosynthesis such as *Acer pseudosieboldianum, Carpinus cordata* (no-la-do-de-ct-ph) and mesophyllous *Alnus hirsuta, Ulmus laciniata* (me-la-do-de-ct-ph). The same trend among PFEs is mirrored in Table 5 for phanerophytes (ph), notophyll leaf size (no) and plants with cortical photosynthesis (ct). Traits matched against Bioclim variables show a common trend in which displacement patterns between present climate and the year 2100 are strikingly similar among the numerous significant correlations. Fig. 2 A, B provides two examples (green stem photosynthesis and PFC) matched against mean minimum moisture index of the driest quarter. Correlations between PFTs (Table 6) and PFEs (Table 7) and the differences in MAP under climate change show some parallels with the patterns in Tables 4 and 5, but with much higher correlation coefficients. In Tables 4 and 6, deciduousness (de) is frequent across PFTs (see above) where, depending on the modal configuration, it is both high negatively and positively correlated but bears little statistical significance when used alone in Tables 5 and 7. It is clear from these results that the functional significance of (de) needs to be considered within the whole-plant modal context rather than as an isolated functional entity.

3.2. Eastern Himalaya, Bhutan

Vegetation recorded from 4,400 m to 340 m elevation covers an exceedingly wide range of types from alpine scree and meadow to lowland seasonal forests bordering the Indian Terai on the Brahmaputra

Table 7
Regional Plant Functional Element (PFE) response to differences in mean annual precipitation under the two climate change scenarios (1975–2100) ordered according to Table 1 and highest correlation values.*

PFE	R.F.E.	Bhutan	Indonesia	Gobi	Namib
pi	0.639 (39.0)	–	–	–	–
le	–	0.522 (27.3)	–	–	–
na	0.505 (23.1)	0.643 (40.1)	–	–	−0.687 (44.8)
mi	–	–	–	–	−0.658 (40.8)
no	−0.823 (66.7)	–	–	−0.492 (21.9)	–
me	−0.632 (38.1)	−0.609 (35.8)	0.531 (26.5)	–	–
pl	–	−0.439 (17.5)	0.517 (25.1)	–	–
ve	0.651 (40.6)	0.440 (17.6)	–	–	−0.738 (52.4)
la	−0.664 (42.2)	–	0.519 (25.3)	–	–
pe	–	−0.526 (26.0)	–	–	–
co	−0.514 (24.1)	–	–	–	–
do	–	–	0.461 (19.4)	–	−0.793 (61.2)
de	–	0.801 (63.4)	–	–	–
ct	−0.805 (63.7)	−0.438 (17.4)	0.466 (20.0)	–	–
ro	–	0.436 (17.3)	–	–	−0.605 (33.8)
pv	–	–	–	–	−0.653 (40.0)
ph	−0.831 (68.1)	–	0.473 (20.6)	−0.501 (22.9)	–
ch	–	−0.547 (28.4)	–	–	−0.606 (33.9)
hc	–	–	–	–	−0.836 (68.6)
cr	–	0.578 (31.9)	–	–	–
th	–	–	–	–	−0.605 (33.8)
li	−0.671 (43.3)	−0.665 (43.0)	0.407 (14.6)	–	–
ep	–	−0.602 (34.8)	–	–	–

* Pearson *r* values show direction of correlation with adj. r^2 % in parenthesis. All $P < 0.005$.

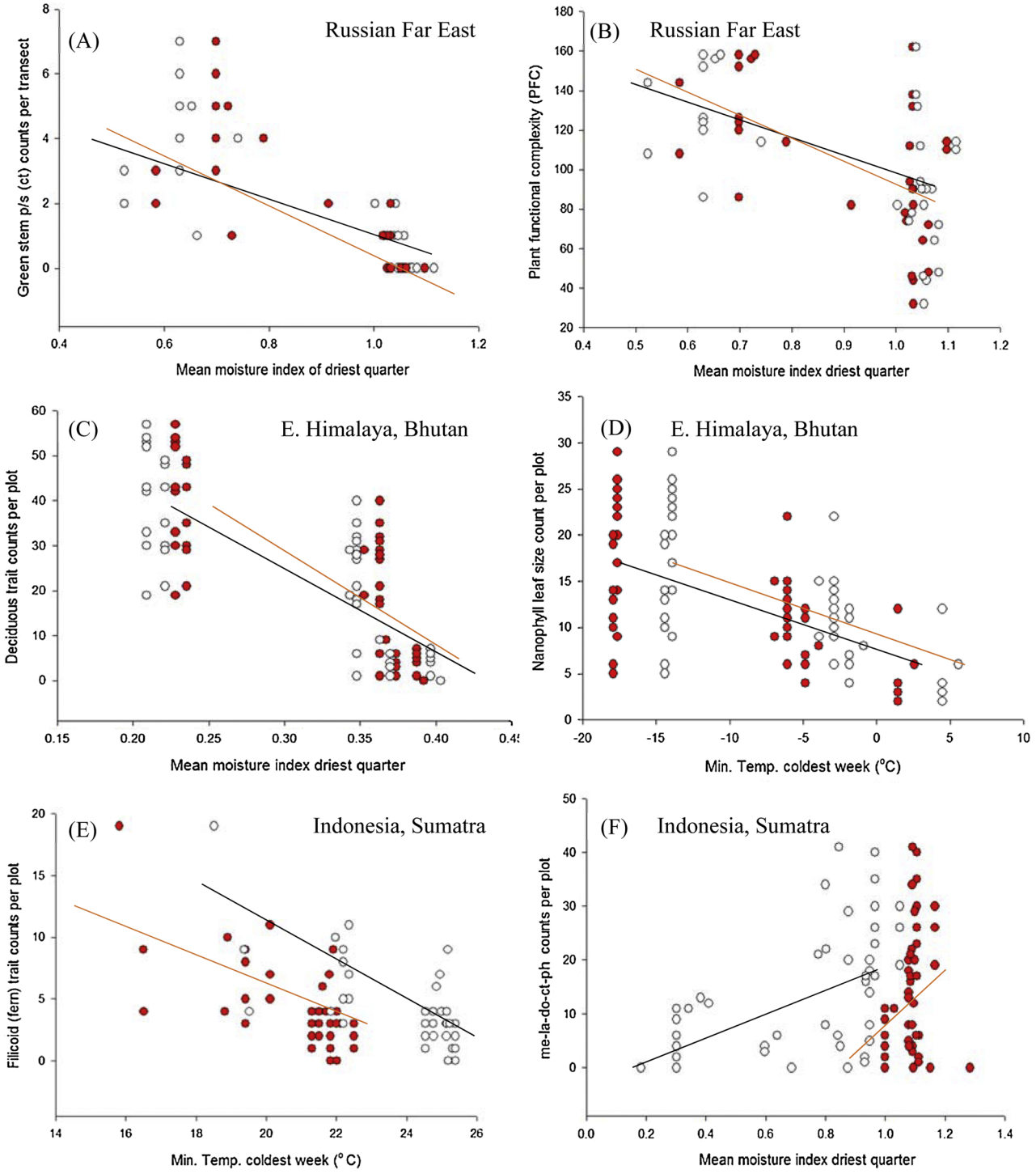

Fig. 2. Examples of trait, PFT (*modus*) and plant functional complexity (PFC) change under climate (red = present climate, white = year 2100) (A) red, adj r^2 = 0.65, $P < 0.0001$; white, adj. $r^2 = 0.67$, $P < 0.0001$ (B) red, adj $r^2 = 0.28$, $P < 0.0009$; white, adj. $r^2 = 0.31$, $P < 0.0001$ (C) red adj $r^2 = 0.28$, $P < 0.0001$; white, adj. $r^2 = 0.31$, $P < 0.0001$ (D) red, adj. $r^2 = 0.36$, $P < 0.0001$; white, adj. $r^2 = 0.36$, $P < 0.0001$ (E) red, adj. $r^2 = 0.44$, $P < 0.0001$; white, adj. $r^2 = 0.45$, $P < 0.0001$ (F) red, adj. $r^2 = 0.23$, $P < 0.302$; white, adj. $r^2 = 0.257$, $P < 0.0002$ (For interpretation of the references to colour in this figure legend, the reader is referred to the web version of this article).

flood plain. The extent of the climate gradient is reflected in the dramatic changes in leaf traits, especially size, inclination and phenology (leaf longevity). This is evident at high elevation in exposed alpine meadows that support leptophylls (le) with lateral inclination (la) such as the ferns *Pteridium revolutum, Athyrium* spp. (le-la-do-de-fi-hc-ad) and the cryptophytic *Acronema tenerum, Pedicularis symphonantha* (le-la-do-de-cr) and vertically inclined *Galium aparine, Gentiana ornata* (le-ve-do-de-hc-ad). At high elevations (>3,000 m) most plants are negatively correlated with annual precipitation. At mid to lower elevations with increasing precipitation, leaf size increases together with lateral inclination, for example *Alnus nepalensis*, *Quercus lamellosa* (me-co-do-ct-ph), *Ribes griffithii* (me-co-do-de-ch-ad), *Nardostachys grandiflora* (me-co-do-de-ro-cr), *Isodon loephanthoides, Rhododendron campylocarpum* (no-la-do-ch) and deciduous *Lyonia villosa, Senecio cappa* (no-la-do-de-

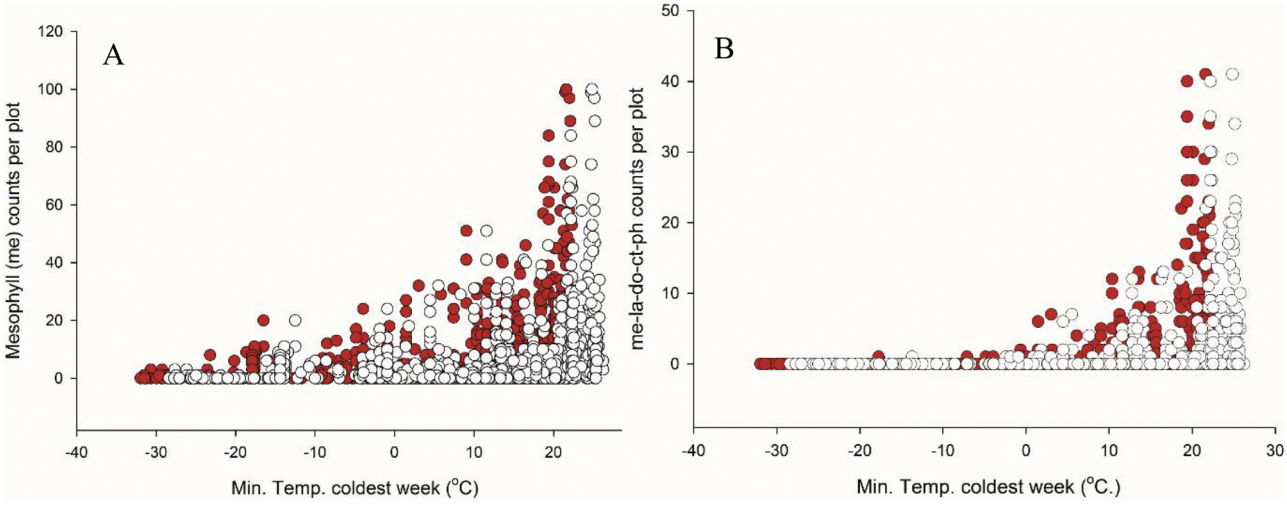

Fig. 3. (A) Global displacement pattern of frequency of plants with mesophyll leaf size and (B) with the modal PFT containing mesophyll leaves when matched against minimum temperature of the coldest week (°C). Red = present climate, white = year 2100 (For interpretation of the references to colour in this figure legend, the reader is referred to the web version of this article).

ch). Along the same gradient, PFTs with rosette phyllotaxy (ro) and vertical leaf inclination (ve) also increase together with epiphytes and lianas. Under both climate scenarios (Tables 4 and 5) with decreasing MAP, a decrease in annuals (therophytes) and cryptophytes is offset by an increase in chamaephytic understorey shrubs. Leaf longevity (deciduousness, de) is characterized by the decrease in the number of PFTs with that trait, being strongly negatively correlated with change and declining steeply with warming and moisture availability, while leaf size is negatively associated with temperature (Fig. 2C,D). When correlated with differences in MAP under climate change (Tables 6 and 7, SI Tables 7 and 8), (de) shows a highly significant positive correlation with decreasing difference in MAP, confirming the trends indicated in Tables 4 and 5. The extreme differences in bioclimate and substrate along the entire gradient preclude a readily generalizeable interpretation of the underlying causes of deciduousness. Severe freezing in the alpine region for example, although driving seasonal leaf fall, is likely to be offset at lower elevations by seasonal dryness (Moisture index driest quarter and maximum temperature CV) rather than by increased warming alone.

3.3. Indomalesia, Indonesia (Sumatra and Java)

Of the five regions, the gradsects selected in Indonesia are relatively less variable in bioclimate. Compared to higher latitudes and the more arid deserts, the humid equatorial region is far higher in floristic and functional diversity or richness (counts per plot). The Sumatran and Javan flora support a wide range of leaf size classes, mostly with lateral or composite leaf inclination. Approximately 16 percent of all PFT records consisted of phanerophytes with green stem (cortical) photosynthesis and mesophyll leaf size, for example *Macaranga hypoleuca, Shorea macroptera* (me-la-do-ct-ph). No significant correlations with MAP were recorded for present climate (Table 4) for these or closely related PFTs. However, plants with mesophyll and platyphyll leaves and cortical photosynthesis (*Artocarpus lancifolia, Neonauclea obtusa* – pl-la-do-ct-ph) were significantly correlated with MAP in year 2100 despite an estimated 19.5% drop in overall precipitation and available soil moisture. Overall, analyses revealed PFTs with larger (mesophyll (me) and platyphyll (pl)) leaves increased under year 2100, as did the number of PFTs with lateral leaf inclination, green stem (cortical) photosynthesis and filicoid ((fi) fern or fernlike) leaves (Fig. 2E,F). Despite the overall decrease in MAP by year 2100, when correlated with decreasing MAP under climate change (Tables 4 and 5), leaf size (me, pl) increases with a corresponding decrease in smaller leaf size (le, na). When compared with the results in Tables 4 and 5 under fixed climate scenarios, correlations with differences in MAP are much stronger in Tables 6 and 7, where, despite the net loss in moisture availability, the correlates maintain a positive trend, notably in increased values in PFTs with mesophyll leaves and lateral inclination and cortical photosynthesis (me-la-do-ct-ph, pl-la-do-ct-ph) as well as lianoid life forms (li) (no-la-do-ph-li).

3.4. Gobi cold desert, Mongolia

Analyses of the available limited climate data indicate a relatively minor response to climate change compared to that of the other regions (Table 8, SI Tables 7 and 8). Available moisture is clearly a dominant factor in plant adaptation to desert environments and consistent with a very positive response of certain modal PFTs to a rainfall (MAP) gradient that varies little with estimated change in 2100 (Table 4). There is a highly significant correlation between MAP and species possessing

Table 8
Global and regional trends for five key Bioclimate variables from year 1975 to year 2100.*

Region	Min. temp. coldest week (°C)	Max. temp. warmest week (°C)	Annual precipitation (mm yr^{-1})	Moisture Index (MI) driest quarter	Radiation warmest quarter (W m^{-2})
Global	3.6	5.5	−1756	−0.15	13.7
R.F.E.	5.9	4.7	62	−0.01	0.5
Bhutan	3.3	6.5	−95	0.01	19.9
Indonesia	3.1	4.4	−439	−0.34	8.7
Gobi desert	4.1	4.2	5	0.0	1.1
Namib desert	3.6	6.4	−48	−0.02	27.6

* Difference in mean values drawn from SI Table 7.

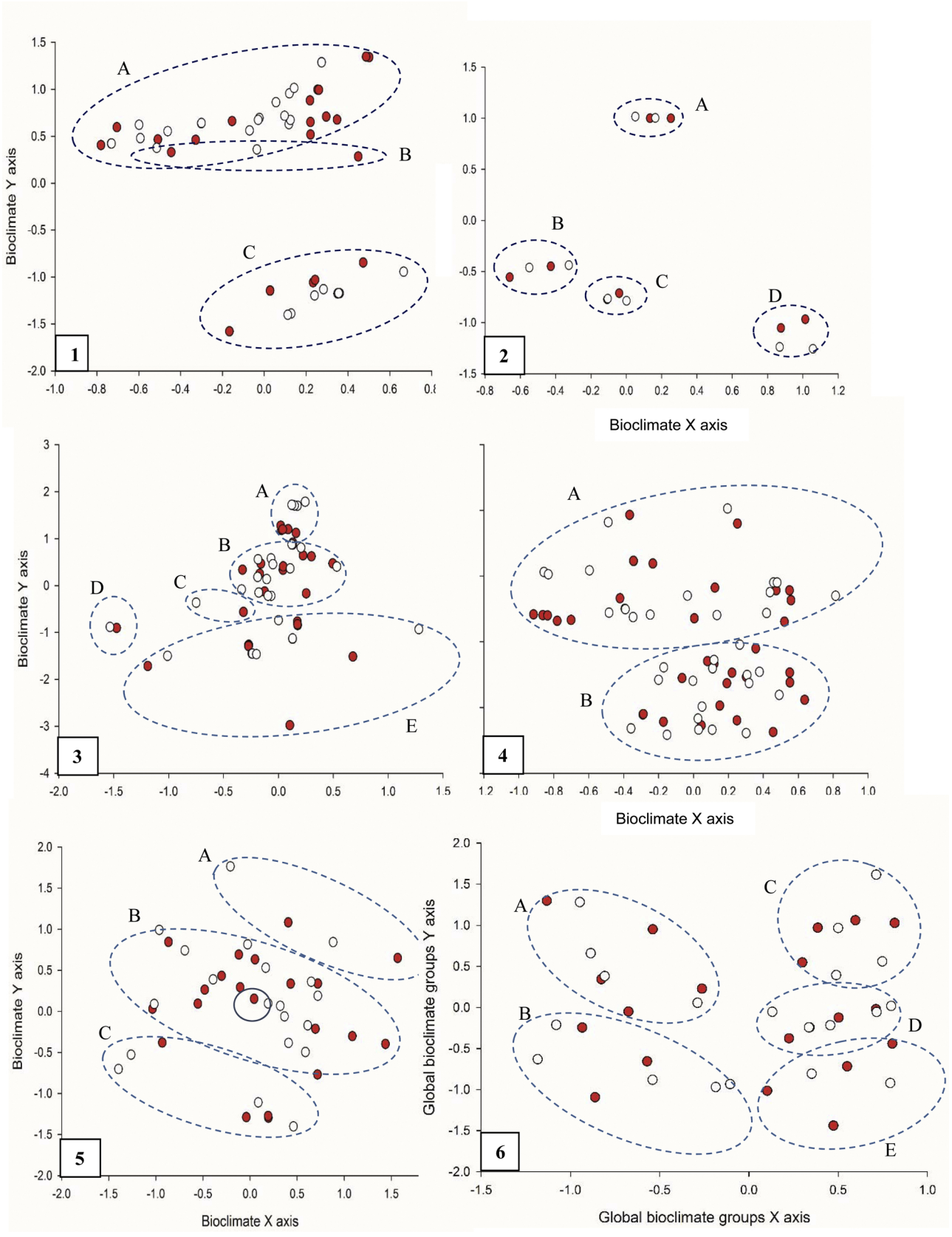

(caption on next page)

Fig. 4. Russian Far East (Kamchatka, Vladivostok) (A) Mixed Alpine tundra *Ledum-Loiseleuria-Vaccinium*, subalpine scrub and conifer-deciduous broadleaf *Pinus-Larix-Betula* woodland (B) Lowland Megaherb field *Angelica-Heracleum*, Dune *Artemisia-Elymus* sward, Tall closed deciduous broadleaf *Populus* forest (C) Lowland Tall broadleaf-conifer *Abies, Picea, Pinus-Quercus* and tall mixed deciduous broadleaf *Fraxinus, Juglans, Ulmus* forest. See main text for related PFTs. Graph of two-dimensional ordinations of eight Bioclim variables. Red = present climate, white = year 2100. 4.2 E. Himalaya, Bhutan (A) Alpine and subalpine mixed asteraceous meadows and *Salix- Juniperus* shrubland with low *Juniperus-Abies-Betula-Acer* conifer-broadleaf forest (B) Montane mixed *Rhododendron-Salix* shrubland with tall *Abies-Larix-Betula* mixed conifer-broadleaf forest (C) Mid to low montane very tall *Picea-Pinus-Castanopsis-Quercus* mixed conifer-broadleaf forest and secondary growth (D) Lowland mainly mixed semi-deciduous *Adenanthera-Acacia-Alnus- Shorea* broadleaf forest with secondary growth. Graph of two-dimensional ordinations of eight Bioclim variables. Red = present climate, white = year 2100. The reduced number of sites displayed is due to overlapping of many site locations that are compressed due to the extreme range of elevations (≈300–4600m). 4.3 Indonesia (Java, Sumatra) (A) Coastal floodplain forest (Myrtaceae, Moraceae, Araceae, Sapindaceae) (B) Agroforests, *Acacia mangium* plantation, Jungle rubber (*Hevea brasiliensis*), *Paraserianthes falcataria* plantation, secondary forest (C) Primary upland forests (Lauraceae (*Litsea*), Fagaceae (*Lithocarpus, Quercus*)) (D) Vulcanoseral heath (Ericaceae (*Rhododendron, Vaccinium*), Bignoniaceae, Melastomataceae, Dipteridaceae (E) Mixed lowland mostly logged forest with dipterocarps (*Hopea, Shorea, Vatica*) and upland primary forests (Fagaceae (*Castanopsis, Lithocarpus*), Cunoniaceae, Lauraceae, Proteaceae). Graph of two-dimensional ordinations of eight Bioclim variables. Red = present climate, white = year 2100. 4.4 Gobi cold desert, Mongolia (A) Mixed tall and open conifer-broadleaf forest (*Larix, Betula, Ulmus*) alpine herbfield (*Oxytropis, Poa, Saussurea*), shrub and open grassland savanna (*Elymus, Stipa, Artemisia*), tussock grassland with succulents (*Elymus, Phragmites, Kalidium*) (B) Grassland steppe (*Stipa, Dontostemon, Asparagus*), Cryptophytic steppe (*Allium, Stipa, Ajania*), short shrub steppe (*Artemisia, Ephedra, Oxytropis, Zygophyllum*), Tall shrubland (*Tamarix, Haloxylon*). Graph of two-dimensional ordinations of eight Bioclim variables. Red = present climate, white = year 2100. 4.5 Namib hot desert, Namibia (A) Tall shrubland *Acacia erioloba* dominant with succulents (*Catephractus, Blepharis, Tribulus, Cleome, Adenolobus*) (B) Mixed short grass and low shrub steppe with many succulents (*Eragrostis, Blepharis, Brownanthus, Zygophyllum*, *Acanthosicyos*) includes *Welwitschia mirabilis* (circled) (C) Mixed riparian shrubland (*Phragmites, Tamarix*). Graph of two-dimensional ordinations of eight Bioclim variables. Red = present climate, white = year 2100. 4.6 Two-dimensional ordination of 20 bioclimate groups matched subjectively against vegetation types. (A) Mainly arctic-boreal tundra and cool-temperate alpine and sub-alpine meadows and shrubland with conifer and deciduous broadleaf forests (B) Mixed dry seasonal desertic and arid grass and shrub steppe with many succulents (C) Highly complex, mainly lowland rainforests and coastal wetlands mixed secondary vegetation mosaics (D) Humid seasonal upland forests with sclerophylls (E) Mainly cool-temperate seasonal vegetation forests and upland savannas (Refer Table 9 for detail and match with modal PFTs). Red = present climate, white = year 2100. (For interpretation of the references to colour in this figure legend, the reader is referred to the web version of this article).

Table 9
Classification of 20 global bioclimate groups matched against indicative modal PFTs.

Group No.	Indicative climate	Key regions	Indicative modal PFTs
1	Arctic boreal	Sweden, Norway, RFE (Kamchatka)	pi-ve-is-ch, le-ve-do-de-ch, na-ve-do-de-hc, mi-ve-do-de-ro-cr
2	Cool temperate seasonal	Baltic, N. Spain, C. Caucasus, N America, Canada, Tasmania (?)	le-co-is-ct-ph, na-ve-do- mi-co-do-pv-th, mi-la-do-de-cr
3	Temperate, moderate seasonal to maritime	China, New Zealand, Macquarie Is., (Subantarctic) UK, N. Spain, Switzerland, Argentina (T. del Fuego), Tasmania	na-ve-do-de-ct-ph, no-la-do-de-ch, mi-la-do-ch, no-la-do-ch-li
4	Cool tropical, subtropical	S. America, Peru, Venezuela, N. America, Cameroun	me-la-do-ct-ph, me-co-do-ct-ph, mi-ve-do-ct-ph, no-la-do-ro-pv-ph
5	Tropical montane, boreal	Kenya (Upland), Vladivostok RFE, Venezuela (Andean)	le-ve-do-pv-hc, na-ve-do-ch, mi-ve-do-pv-hc, me-la-do-de-ct-ph
6	'Mediterranean'	S. Spain, Sicily, S. Africa, W. Australia	pi-ve-is-so-su-ch, le-ve-do-hc, na-ve-do-hc, na-ve-do-ch,
7	Semi-arid to desertic	Arizona, W. NSW, Queensland	pi-ve-is-ct-ph, na-ve-is-ch, mi-pe-is-ct-ph, mg-ve-is-so-su-ct-ph,
8	Tropical to sub-tropical	S. America (Brazil, Guyana, S.E. Mexico), S.E. China, Vietnam, S. Thailand, Philippines, S.E. Africa	mi-co-do-ct-ph, no-la-do-ct-ph, me-la-do-ro-pv-ph, pl-ve-do-su-ph,
9	Humid seasonal tropical	E. Queensland coastal and upland	no-la-do-ph, me-la-do-ro-pv-ph-ad, pl-la-do-ct-ph, ma-la-do-su-pv-hc-ep
10	Humid tropical	Upland NE Australia	no-la-do-ct-ph, no-ve-do-ph, mi-la-do-ro-fi-ph-ad, no-pe-is-ct-ph
11	Warm semi-arid to desertic, strongly (drought) seasonal	Mali, Namibia, Dubai, Spain, Tenerife, N. Thailand, Mozambique, SW Australia, NW Queensland	mi-pe-do-de-ch, mi-ve-do-th, mi-co-is-ct-ph, no-ve-is-su-ch
12	Cool temperate seasonal	Bhutan (Montane)	na-ve-do-de-ch, na-ve-is-so-ch, me-ve-do-de-hc, mi-pe-do-de-cr
13	Temperate, seasonal	Assam, Nepal, Bhutan (lower montane)	na-co-do-de-ph, mi-co-do-pv-hc, no-pe-do-de-ct-ph, pl-la-do-ct-ph,
14	Continental cold desert	Mongolia (Gobi)	pi-ve-is-de-so-su-hc, mi-pe-do-de-ct-ph, mi-ve-do-de-ro-cr,
15	Cool temperate, seasonal	Bhutan (high montane, subalpine), E. Himalaya	le-ve-do-ch, le-ve-is-de-so-su-ch,mi-ve-do-de-ct-ph, mi-la-do-de-hc-ad, pl-la-do-de-cr,
16	Humid tropical, oceanic	Indomalesia, Borneo, Indonesia, Oceania New Guinea, Fiji, New Caledonia, Peru, Guyana (lowland)	me-la-do-ph, no-la-do-ct-ph, no-la-do-ph-li-ad, ma-la-do-ro-ph
17	Humid tropical semi-maritime	Indonesia, Java	me-la-do-ro-pv-ph-ad, no-la-do-ct-ph, mi-ve-do-ct-ph, no-ve-do-ph
18	Tropical moderately seasonal	Peru (lowland Amazon basin)	na-la-do-de-ct-ph, me-la-do-ct-ph, ma-ve-do-pv-hc-ad, me-la-do-ct-ph, ma-la-do-ct-ph
19	Temperate, semi-arid	S. Queensland	na-ve-is-so-ph, na-ve-do-su-hc, mi-pe-do-ph, no-pe-is-ph
20	Tropical upland mod. seasonal	NE Queensland (upland)	no-ve-is-ct-ph, me-pe-do-ct-ph, no-pe-do-ph-li, mi-co-is-ph

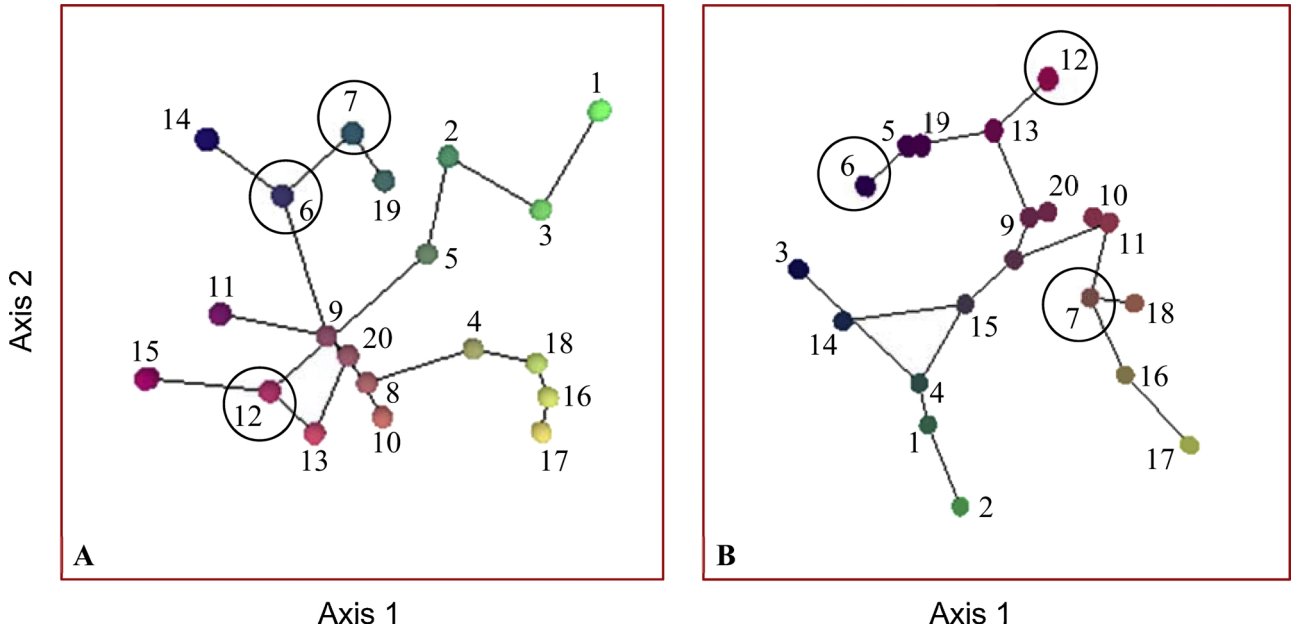

Fig. 5. Two dimensional MDS of 20 classes of global bioclimate based on means of eight bioclimatic variables per class (Table 9). Colours and minimum spanning tree indicate group structure. Circled areas and their trajectories are described in main text (A) Present climate, (B) year 2100.

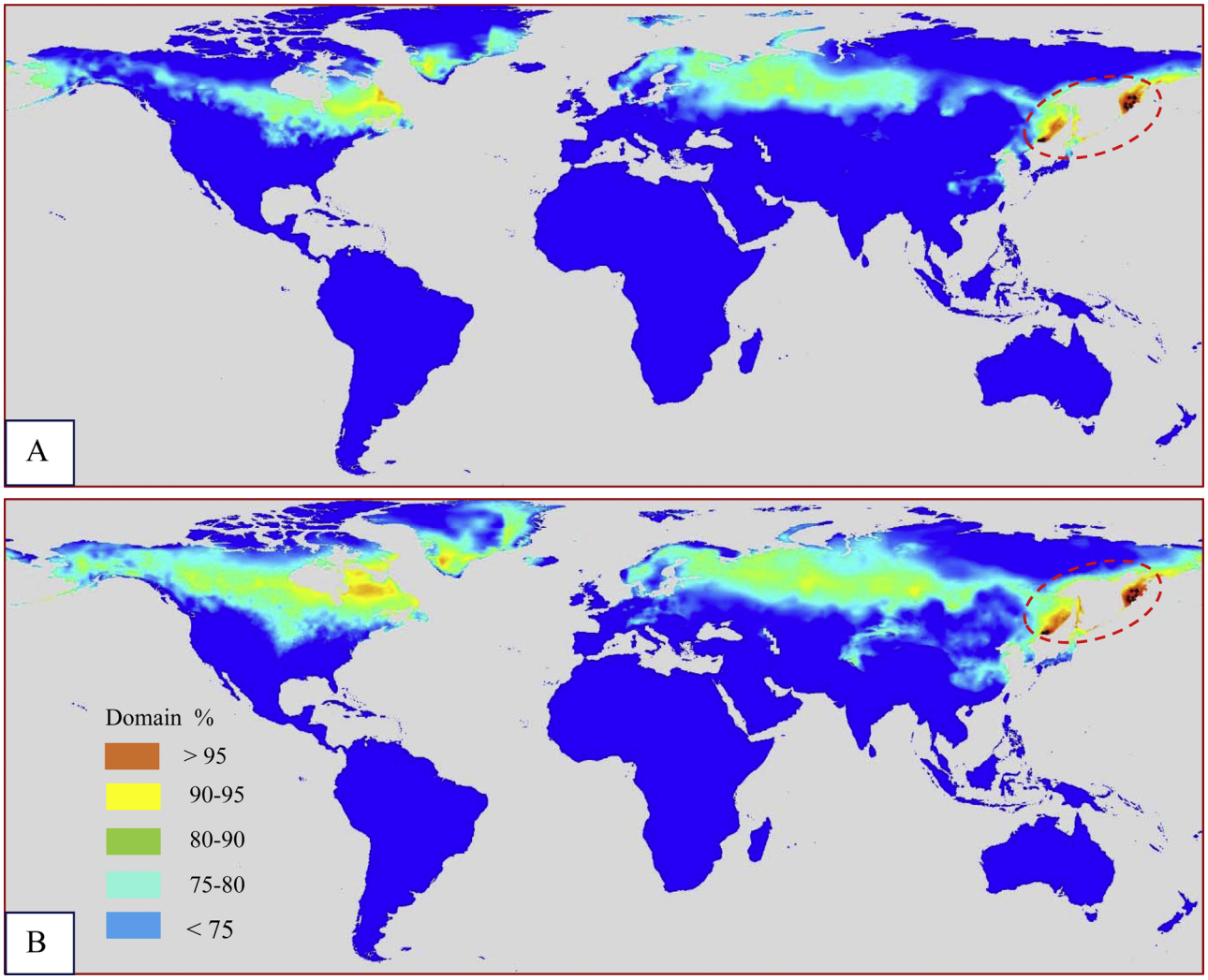

Fig. 6. Spatial model of global climate similarities relative to range standardized sites in the Russian far East based on eight Bioclim variables. (A) present climate, (B) climate for year 2100 (Percent similarities shown in legend with red = 100 percent in Figs. 6–10).

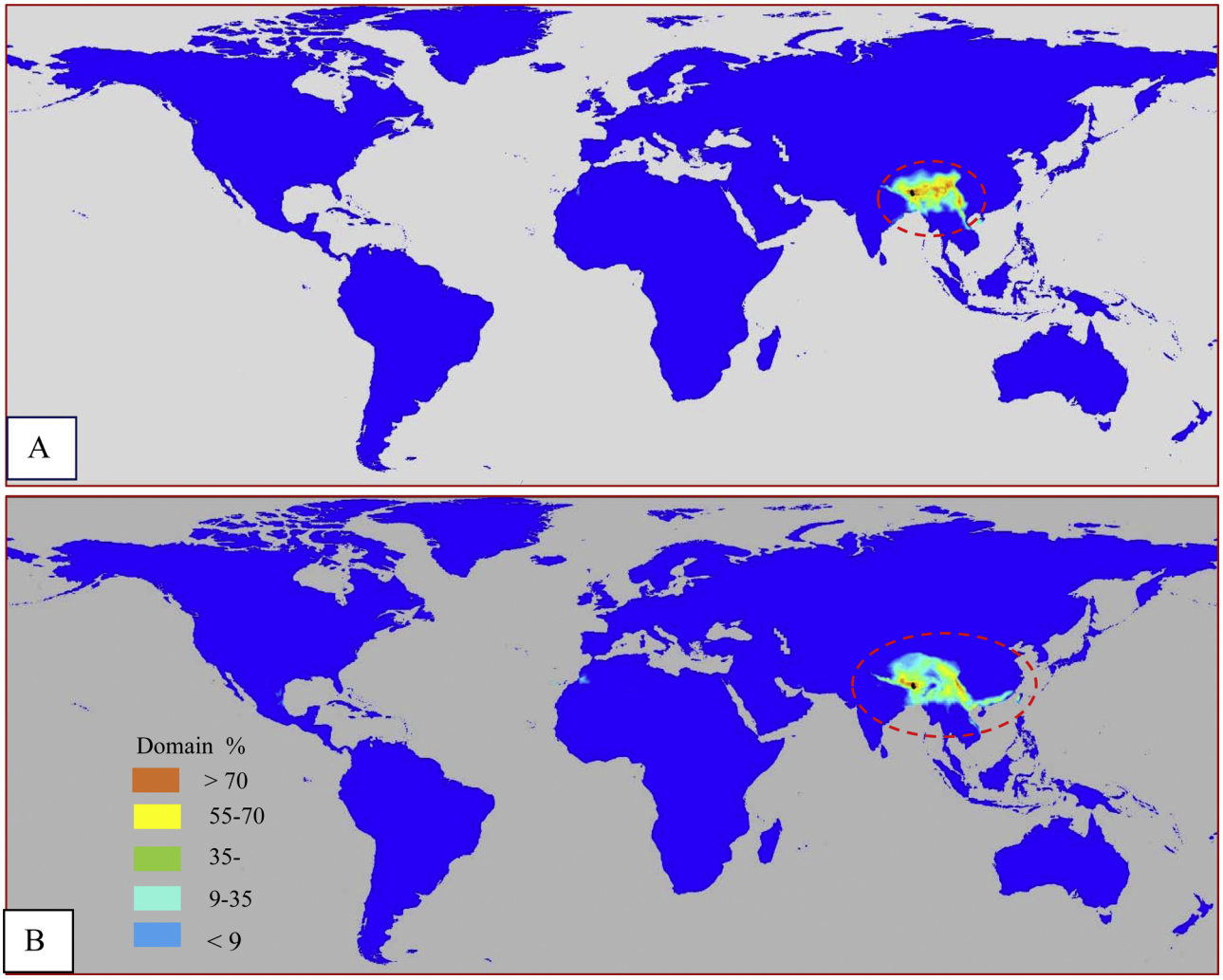

Fig. 7. Spatial model of global climate similarities relative to range standardized sites in the E. Himalaya based on eight Bioclim variables. (A) present climate, (B) climate for year 2100.

modal PFTs with nanophyll (na) and vertically inclined (ve) leaves that are either deciduous or annual (Therophytes) (th) or cryptophytes (cr) (plants with below-ground bulbs or tubers). These are exemplified by *Youngia* sp. (na-ve-do-ch), *Potentilla tanacetifolia* (na-ve-do-de-cr), *Artemisia gmelinii*, *Veronica incana* (na-ve-do-de-hc) and *Poa botryoides* (na-ve-do-de-pv-hc). The Gobi also supports many Chenopodiaceae, notably the 'Saxaul' *Haloxylon ammodendron* (le-ve-is-de-so-su-ch), *Salsola collina* (le-ve-do-de-so-hc), and Tamaricaceae *Reaumuria soongarica* (pi-ve-is-de-so-su-ph) that represent many taxa with succulent and solidiform leaf adaptations to seasonal aridity. These PFTs and their individual PFEs that characterise this continental desert, differ markedly from the other regions. The taxonomic and PFT data do not reveal, however, that in the Gobi desert (as well as upland E. Himalaya) available moisture is also governed to a large extent by aspect on hill slopes, implying caution when using PFTs as indicators of vegetation response to climate change at landscape level. While the correlative values under each climate scenario show some highly significant relationships, these disappear when comparisons are made in Tables 6 and 7 with little or no correlation when probabilities are limited to $P < 0.005$. This result is almost certainly due to the very marginal values in precipitation change. Compared to the other regions, species and PFT richness together with PFC have the highest correlations with ordination values of Bioclimate (SI Table 4).

3.5. Namib hot desert, Namibia

Unlike the lower temperatures of the Gobi desert, the Namib is classified as a 'hot' desert with temperatures exceeding 45 °C in the central Namib although nights can be cold (2.3 °C, SI Table 7). As with the Gobi desert, modal PFTs are most frequently chamaephytic shrubs with nanophyllous and microphyllous (na, mi), vertically inclined (ve), hypostomatous (mainly (do)) leaves such as *Blepharis grossa, Catoephracteus alexandri* (na-ve-do-ch) and *Adenolobus pechuelii* (mi-ve-do-ch), both PFTs that are highly correlated with annual precipitation (Table 4). Smaller picophylls (pi) are frequent in Mimosaceae (*Vachellia* and *Senegallia* spp.) (pi-ve-do-ch), while leptophylls (le) such as *Mesembryanthemum kuntzei* (le-ve-is-so-su-ch) and microphyllous (mi) *Tetraena stapffii* (mi-ve-do-is-su-so-ch) typify many succulent (su) taxa with solidiform (so) isostomatous leaves adapted to arid conditions. The PFT and PFE correlates in Table 4 and 5 bear little comparison to the precipitation values under climate change (Tables 6 and 7) where there are strong indicators in both modal PFTs and PFEs, and where Namibian PFEs are much more strongly correlated with differences in MAP than the PFEs in the Gobi desert. In the central Namib desert mention should be made of the remarkable megaphyllous (mg) *Welwitschia mirabilis* which is an extremely unique adaptive form (mg-co-is-pv-ch). Unlike the more seasonal Gobi desert, the majority of plants in the Namib are evergreen rather than deciduous with fewer annuals and cryptophytes recorded in this study.

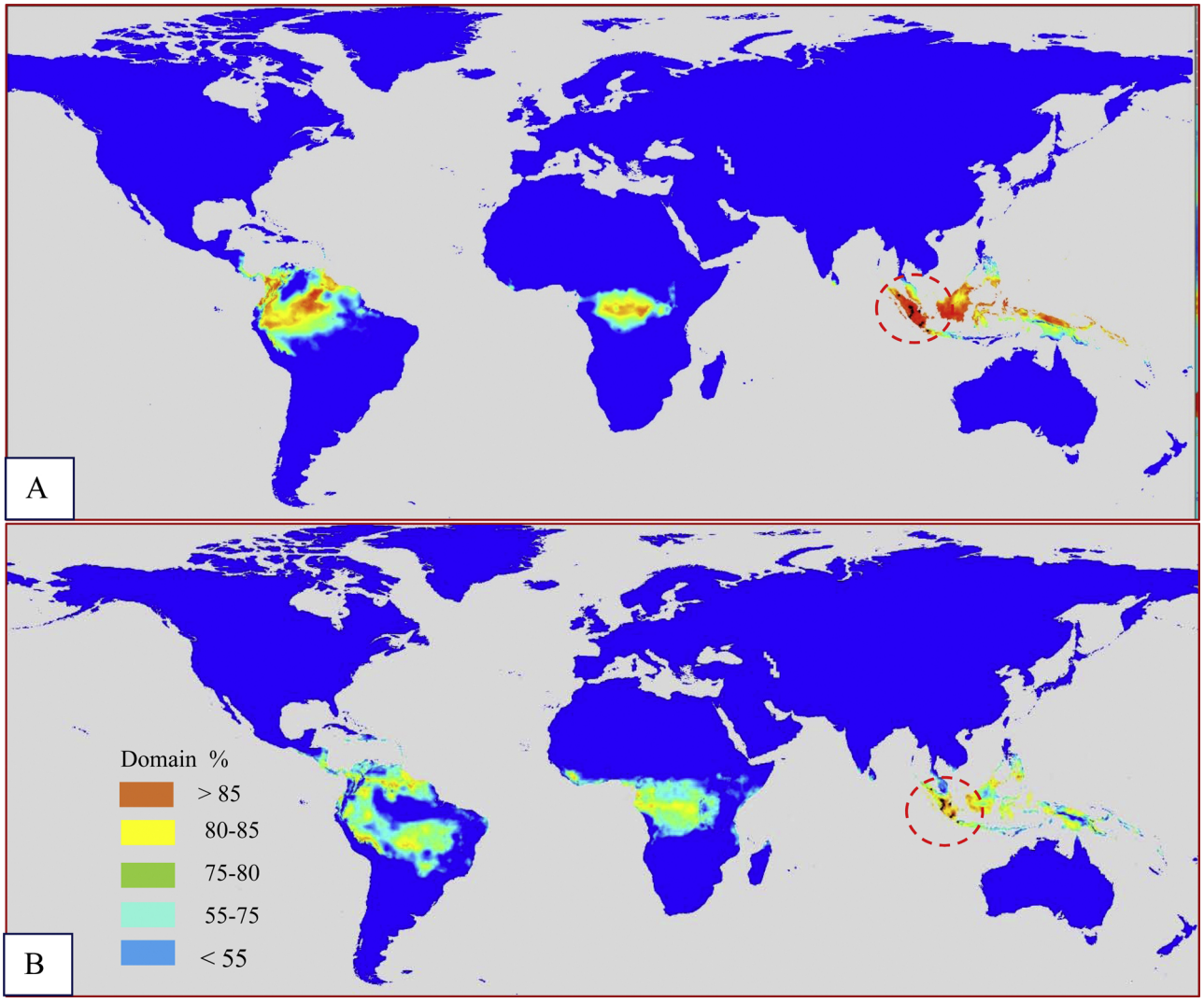

Fig. 8. Spatial model of global climate similarities relative to range standardized sites in Indomalesia (Indonesia) based on eight Bioclim variables. (A) present climate, (B) climate for year 2100.

3.6. Regional and global trends

Global changes in bioclimate indicate general warming with a substantial decrease in annual precipitation (Table 8, SI Table 7). However, this is not reflected in individual regional response patterns where, although all regions show a distinct warming trend with limited increases in MAP in the RFE and Mongolia, there are significant decreases in Indonesia and, significantly, Namibia. Perhaps more significantly for plants, is a decrease in moisture availability especially in the driest quarter, across all areas except the relatively stable Gobi desert. In the E. Himalaya of Bhutan, the many similar highly significant correlations between PFEs and PFTs for both climate scenarios may not reflect a true picture of vegetation response in that very environmentally and topographically complex region. For Bhutan at least, preliminary analyses indicate that more meaningful changes under both climate scenarios become evident if data are stratified according to altitudinal subsets and analysed separately. Regional floristic and plant functional diversity (richness) vary with climate change (Table 3). In the RFE species and PFT richness and PFC change in a consistent pattern from present to future climate while there are no significant indicators for the E. Himalaya (again possibly due to loss of environmental signal masked by extreme elevational range). In Indonesia, species and PFT richness and PFC decrease with temperature, while both desert regions show a positive correlation with MAP despite a significant drop in precipitation and moisture availability in the year 2100 for the Namib (SI Tables 7 and 8). At global scale many PFTs and PFEs exhibit a non-linear relationship with certain bioclimate variables under both present and future climate. An example of such a relationship (Fig. 3) is illustrated between minimum temperature of the coldest week and plants with mesophyll leaf size class (Fig. 3A) and modal PFTs possessing that trait (Fig. 3B).

The grouping of vegetation types displayed in Fig. 4 is the result of multidimensional scaling of the eight Bioclim variables expressed in two dimensional space across regional and global scales (Fig. 4). Within the groups described, with some slight exceptions (Fig. 4) there is little to suggest any significant response in pattern to climate change in groupings in Fig. 4. Rather, the ordinations provide instead a multidimensional framework whereby vegetation patterning can be subjectively linked with bioclimate under the two climate scenarios. Higher level matching between bioclimate and modal PFTs at global scale (Fig. 4.6) can be seen with an ordination of the mean bioclimate variables of 20 bioclimate groups (Table 9) that were classified and ordinated according to the 8 global bioclimate variables. A two-dimensional ordination of 20 classified global bioclimates (Fig. 4.6) produced five recognizeable subgroups of broad vegetation types. Matching modal PFTs against these 20 bioclimate groups (Table 9) revealed a distinctive trend in both PFT and PFE association with bioclimate at this level. Because unique modal PFTs across groups are very

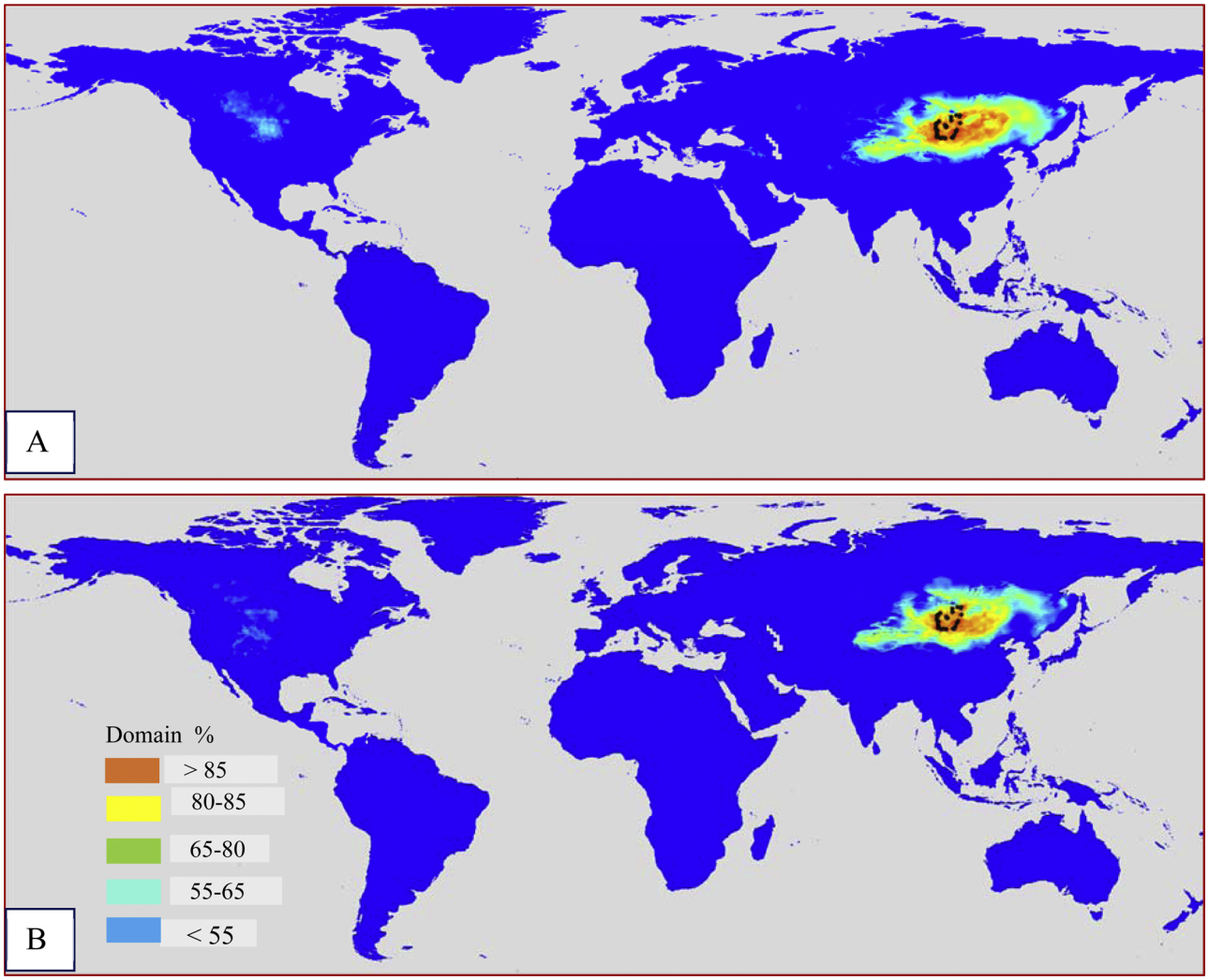

Fig. 9. Spatial model of global climate similarities relative to range standardized sites in the Gobi hot desert (Outer Mongolia) based on eight Bioclim variables. (A) present climate, (B) climate for year 2100.

numerous, for presentation purposes four PFTs per group were subjectively selected as being indicative of each group (examples in parentheses below). Within this classification, PFTs with Raunkiærean life forms are widely distributed across the full global spectrum but with higher frequencies of hemicryptophytes (hc), chamaephytes (ch) and cryptophytes (cr) at higher (cooler) latitudes and elevations and with increasing aridity (reflected in minimum temperature of the coldest week and CV of soil moisture index). Also associated with these extremes are mainly chamaephytic (ch) PFTs with typically very small leaf size (picophyll (pi), leptophyll (le)), vertical leaf inclination (ve) and isostomatous leaves (is) (pi-ve-is-ch, pi-ve-is-ct-ph, pi-ve-is-su-so-ch, le-co-is-ct-ph) (groups 1, 2, 6, 7 in Table 9). While deciduousness (de) is most frequent in groups 1, 2, 3, succulence (su) and solidiform (isocentric) (so) forms increase towards desertic environments (pi-ve-is-so-su-ch) (groups 6, 7). Phanerophyte (ph) PFTs with green stem (cortical (ct)) photosynthesis are widespread across these high latitude groups, occurring for example, in certain boreal conifers (*Pinus sylvestris*) (na-ve-do-ct-ph) and deciduous broad-leaved taxa (*Betula pubescens* var. *tortuosa*) (mi-co-do-de-ct-ph). Although widespread in boreal climates, cortical photosynthesis is most evident in arid extremes, especially in Cactaceae (*Carnegiea gigantea*) (mg-ve-is-su-so-ct-ph) and many 'cactoid' forms (*Euphorbia canariensis*) (ma-ve-is-so-su-ct-ph) with similar modal PFTs (groups 7, 11, 14). 'Corticoid' PFTs also occur throughout the seasonal tropics (deciduous Burseraceae, Hernandiaceae, Mimosaceae, Moraceae) (groups 8, 9, 20) as well as the humid tropics where they are found especially in seral, mid- to late stage forest successions and forest canopy gaps (Cercropiaceae, Euphorbiaceae) (groups 16, 17, 18).

While Fig. 4 reveals broad patterns of vegetation response to bioclimate, a more succinct indication of response to climate change is portrayed in Fig. 5 where a network of relative differences in multidimensional relationships between the 20 groups under climate change is presented via a minimum-spanning-tree based on the mean values of each bioclimate variable for each classified group (Table 9, SI Tables 5 and 6). Changing trends in vegetation types under the climate scenario indicated for the year 2100 are indicated in Fig. 5 by examples of changes in the trajectories of groups 6, 7 and 12 and their spatial relationships with other groups. In the regions under study, vegetation least affected by climate change are groups 16, 17, 18 (neo- and paleotropic and equatorial oceanic regions) characterised by mainly humid tropical and mildly seasonal vegetation. Group 7 that is indicative of semi-arid to hot dry deserts (Australian W. NSW and Queensland and the Sonoran desert of Arizona) typified by plants with green-stem photosynthesis and succulent and isostomatous (mainly isobilateral and isocentric) leaf types moves in a trajectory towards vegetation under a warmer, humid climate occupied by groups 16, 17, 18 with larger, more mesophyllous leaves and leaves with lateral inclination. Under climate change, group 6, mainly 'Mediterranean' (S. Spain, Sicily, S. Africa and W. Australia) occupy a more temperate climate with changes from hemicryptophytic and chamaephytic,

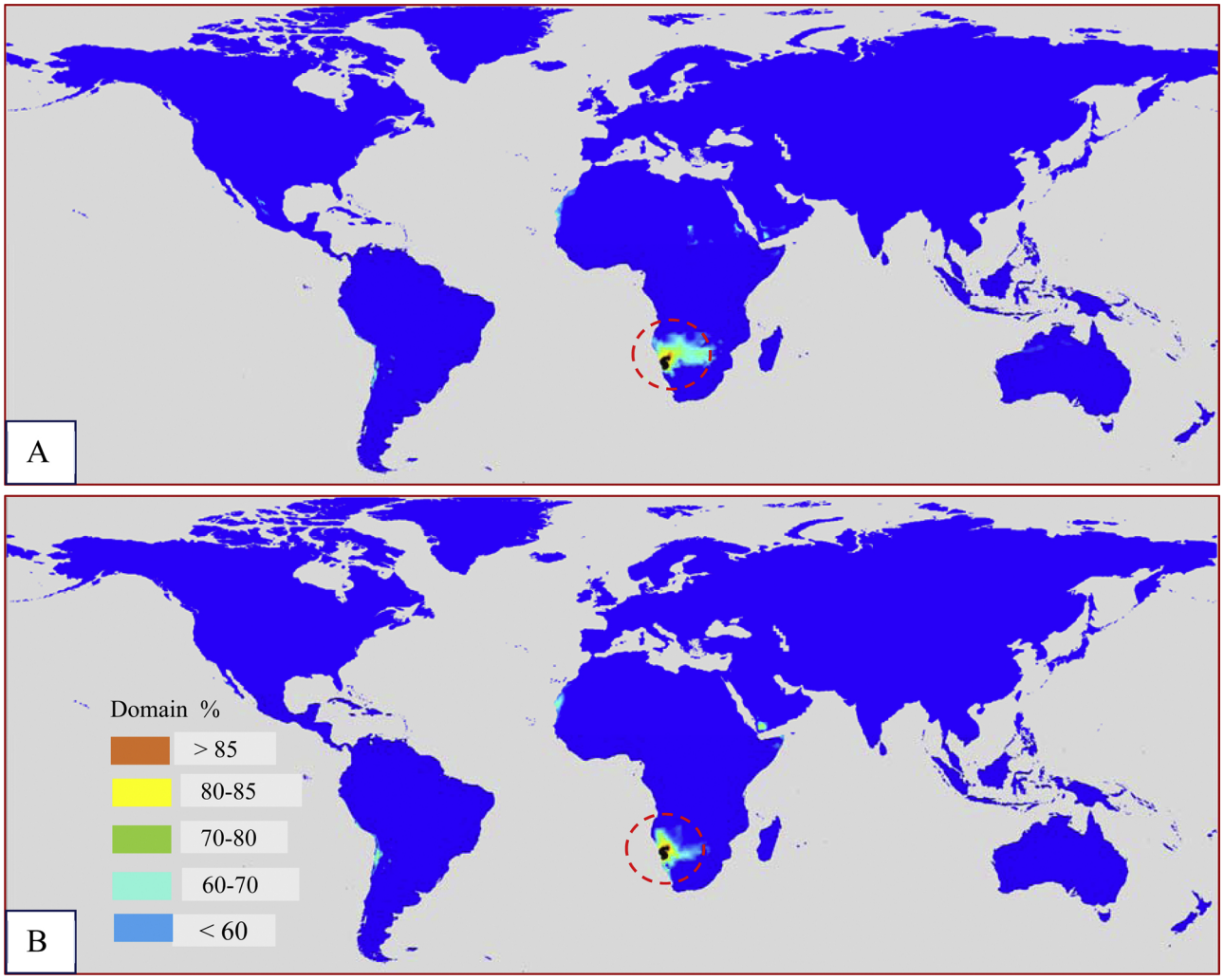

Fig. 10. Spatial model of global climate similarities relative to range standardized sites in the Namib hot desert (Namibia) based on eight Bioclim variables. (A) present climate, (B) climate for year 2100.

shrubby vegetation to one with increasing frequencies of taller phanerophytes. On the other hand, Group 12 (cool-temperate seasonal climate in high montane E. Himalaya) with dominant chamaephytic, hemicryptophytic and cryptophytic vegetation will move towards warmer Group 13 (E. Himalaya lower montane) to be represented by increasing frequencies of phanerophytes and increasing leaf size class. In northern latitudes, under the bioclimates estimated for year 2100, the Arctic Boreal group 1, currently a relatively isolated group under present climate, becomes more closely associated with groups 2 and 4 with more mesophytic, taller vegetation, suggesting a response to significant changes in warming. By comparison, the southern regions are more widely dispersed with partial overlaps between the E. Himalaya and the Indonesian archipelago. Viewed overall, these examples suggest trends away from arid and semi-arid, seasonal sclerophyllous, small-leaved shrubby vegetation types, to climates that support vegetation with fewer hemicryptophytes and cryptophytes (geophytes) and increasing frequency of taller ligneous plants and more mesophytic leaf types.

Spatial modeling of relative regional geospatial changes under climate (Figs. 6–10) indicates considerable expansion of bioclimate warming across all areas in each of the five regions. The most extensive are in high latitudes (Fig. 6B) increasing in northern Europe, Fennoscandia, Greenland and North America, whereas expansion in the E. Himalaya (Fig. 7B) is more constrained possibly due to complex geomorphologies, but extends in a radius that includes coastal massifs in southern China. Areas of increased warming in tropical regions are evident in central and maritime Africa with similar extensions in South America (Fig. 8B). Both the Gobi (Fig. 9) and the Namib (Fig. 10) deserts indicate a moderate increase in the spatial extent of current modal PFTs by the year 2100. The general increase in warming across the African and S. American tropics and sub-tropics is offset by an apparent, but unexplained, general decrease in warming in Indomalesia and parts of Oceania. Pictorial examples (Figs. 11–15) of potential shifts in vegetation types under climate change are relatively consistent with the results of the regional data analyses and, apart from evident differences in vegetation canopy and life forms, indicate significant changes in vegetation structure and physiognomy. When considered at global scale (Fig. 16A and B) overall changes in bioclimate are consistent with patterns of increased warming evident in the five regions, with the most significant again being likely in high northern latitudes. The relative contribution of modal PFTs to the pattern of global bioclimate (Table 10) indicates that, in the 3403 unique PFT combinations identified in the global dataset, there is a decline from larger (e.g. mesophyll) leaves to those of smaller size and from lateral to vertical inclination, all with dorsiventral leaves indicating a dominance of leaves with mainly abaxial stomatal (hypostomatous) adaptation. This global distribution pattern is consistent with increased floristic richness in humid equatorial regions (Hillebrand, 2004; Mittelbach et al., 2007) and leaf functional performance, despite some evidence for a mid-latitude spike (Gillison, 2016, 2018). Dominant woody life forms

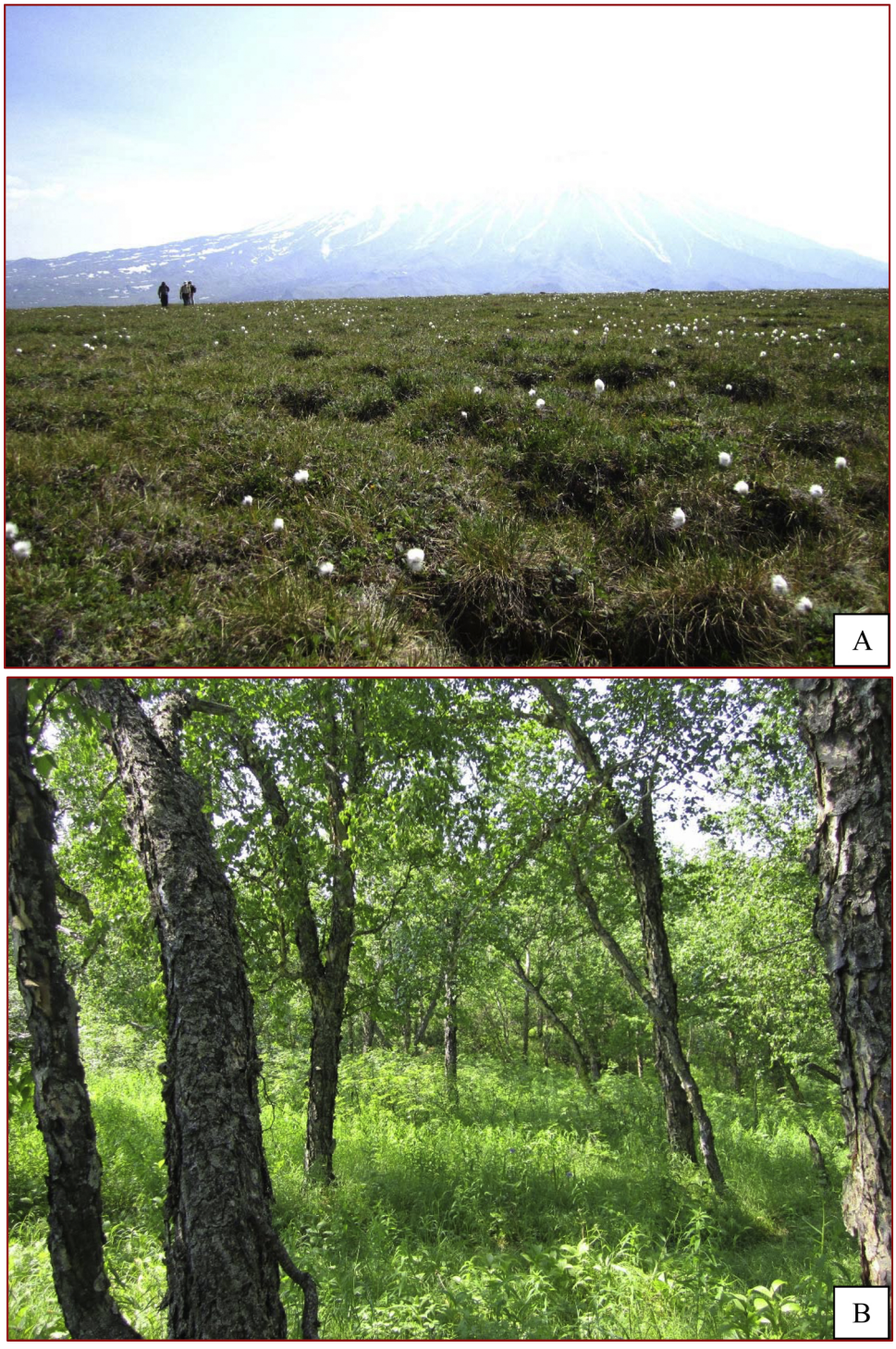

Fig. 11. Potential change in vegetation types from (A) present day dry tundra near Mt Plotskaya, Kamchatka RFE (Elevn. 1417 m, from -29.3 to -21.9 °C Min T. coldest month predicted for year 2100, towards (B) deciduous broadleaf forest (Stone Birch, *Betula ermanii*) and mixed broadleaf conifer forests (Elevn. 847 m, present day -23.6 °C).

decrease from phanerophyte to chamaephyte in frequency, many with lianoid form, to more herbaceous (hemicryptophyte) graminoid types. Of particular significance is the global dominance of PFTs exhibiting green stem or cortical photosynthesis that occupy almost 7.5 percent of the world's flora in this study. The dominance of certain PFEs is generally consistent with the dominant PFT listing. For example, the PFEs that constitute the dominant PFT (*me-la-do-ct-ph)* (Table 10) contain almost 45 percent of the PFEs recorded for the world's flora.

4. Discussion

The preceding paper (Gillison, this volume) reviewed the use of individual functional traits (FTs) and Plant Functional Types (PFTs) as potential indicators of vegetation response to climate change with respect to their characterisation of whole-plant fitness. This paper has addressed the hypotheses raised in the preceding paper through an analysis of global data comprising bioclimate-linked modal PFTs. The application of a modal PFT concept in this way does not appear to be

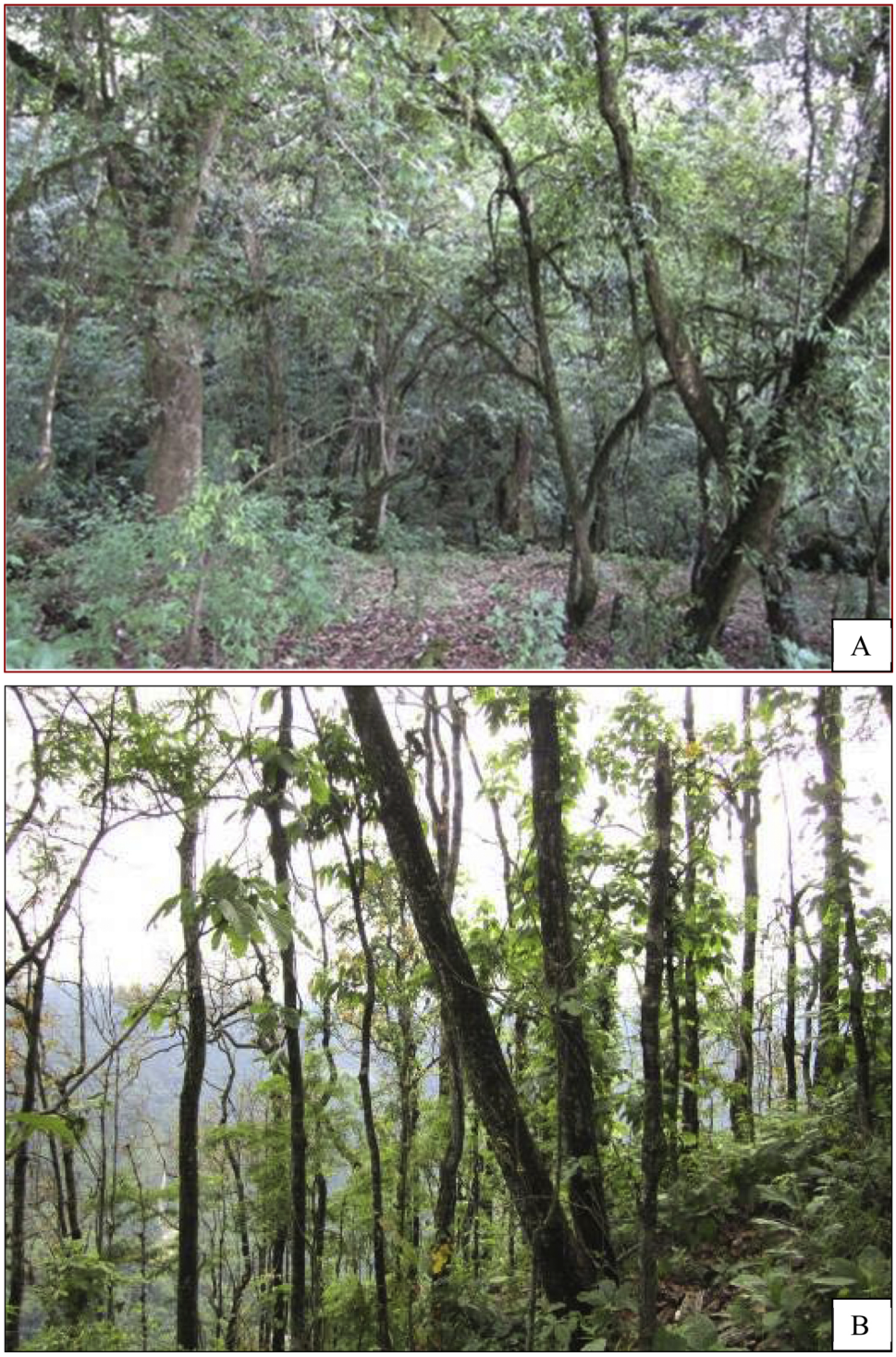

Fig. 12. Potential change in forest structure from (A) present day upland Tall semi-deciduous broadleaf forest in E. Himalaya (Bhutan) (Elevn. 2800 m, from -4.8 to predicted -1.8 °C Min. T. coldest month in year 2100, towards (B) drier forest types such as Sal (*Shorea robusta*) deciduous forest (Elevn. 1929 m, present day Min. T. coldest month 1.5 °C).

replicated elsewhere and previous work involving a similar concept is difficult to find. A broadly similar approach towards the construction of assembly and response rules for predictive community ecology proposed by Keddy (1992) required access to a comprehensive species pool and measureable traits for each species as in the present treatment. Keddy's procedure involved specifying which traits (and therefore which subset of species) should occur in a particular environment, thereby establishing a basis for predicting the response and re-assembly of functional traits (and species) to environmental change – in his case wetland communities. While some parallels can be drawn with forecasting response to climate change in the present treatment, Keddy's proposal does not appear to be supported by a detailed study using specific trait combinations. A subsequent algorithm for seeking an optimal parsimonious set of traits (Pillar, 1999; Pillar and Sosinski, 2003) enabled predictive coupling between environment and functional types. Although that work was based on a trait set with limited evidence of links with environment, the algorithms developed by Pillar and Sosinski (2003) might well apply to the modal PFTs in the present paper.

Fig. 13. Potential change in forest structure from (A) present day upland mixed fagaceous (mainly *Castanopsis*) forest in Sumatra, Indonesia (Elevn. 1282 m, from 18.8 to predicted 21.8 °C Min. Temp. coldest month) in year 2100, towards (B) more structurally and functionally complex lowland forests with many dipterocarps (Elevn. 780 m, present day Min. Temp. coldest month 19.4 °C).

A more recent investigation (Douma et al., 2012) employed similar criteria to the selection of modal PFTs to those in the present study, namely, that the trait should be directly or indirectly related to plant fitness, well represented in the species pool and allow for comparison with existing strategy schemes. Of the twelve traits selected by Douma et al. (2012) analysed using community means, most required laboratory or very detailed field measurements and included data sourced from a variety of external databases. From their analysis of a very extensive database for the Netherlands flora, Douma et al. (2012) were able to show that, with seven plant traits, functional composition could explain up to 80% of the floristic differences between species assemblages. Especially significant was the conclusion by Douma et al. (2012) that, contrary to expectations, the individual performance of a trait was not a predictor of its performance in combination with other traits – a conclusion consistent with findings in the present study. This finding, which tends to be supported in other work (Schulze, 1982; Marks and Lechowicz, 2006; Pillar, 1999; Pillar and Sosinski, 2003), has significant implications for the use of single versus modal PFTs or similar species-trait sets in predictive modeling of vegetation response to climate change.

Studies involving the use of plant functional types (PFTs) and individual functional traits (FTs) have generated a rich array of literature that focuses primarily on community or laboratory based data sets using parsimonious sets of FTs. Based on their performances at local scale, many of the same FTs are being increasingly applied in dynamic vegetation models at large regional and biome level, often without critical attention to changes in response dynamics across changing environmental scales (*cf*. Van Bodegom et al., 2014). Given the often

Fig. 14. Potential change in structure and composition in the Gobi cold desert, Mongolia from (A) present day desertic short grass steppe with mainly dominant *Agropyron cristatum* and *Convolvulus ammannii* (Elevn. 1462 m, from -24.1 to predicted -20.2 °C Min. Temp. coldest month in year 2100), towards (B) more structurally and functionally complex 'mini-dune' shrub-grass steppe with *Agropyron cristatum, Artemisia subdigitata* and *Salsola collina* (Elevn. 1320 m, present day Min. Temp. coldest month -21.9 °C).

indeterminate response of intraspecific genotypes to environmental change, the specific conditions under which individual traits can be regarded as independent or 'orthogonal' (i.e. not correlated, Ackerly, 2004; Wright et al., 2007) are likely to be better determined only by rigorous experimentation (*cf*. Schimper, 1903). The magnitude of such a challenge presents life scientists with the daunting prospect of devising alternative 'best bet' strategies based to a large extent on available knowledge, in a race to provide baseline data and information to help ensure the maintenance of ecosystem services under climate change.

Building on the arguments and emergent hypotheses presented in the preceding paper (Gillison, this volume), this paper explored the potential utility of one 'best bet' strategy by analysing the functional performance of whole-plant modal PFTs constructed according to a core set functional traits and tested across a series of environmental gradients at multiple scales. Here, 'performance' is defined by the degree to

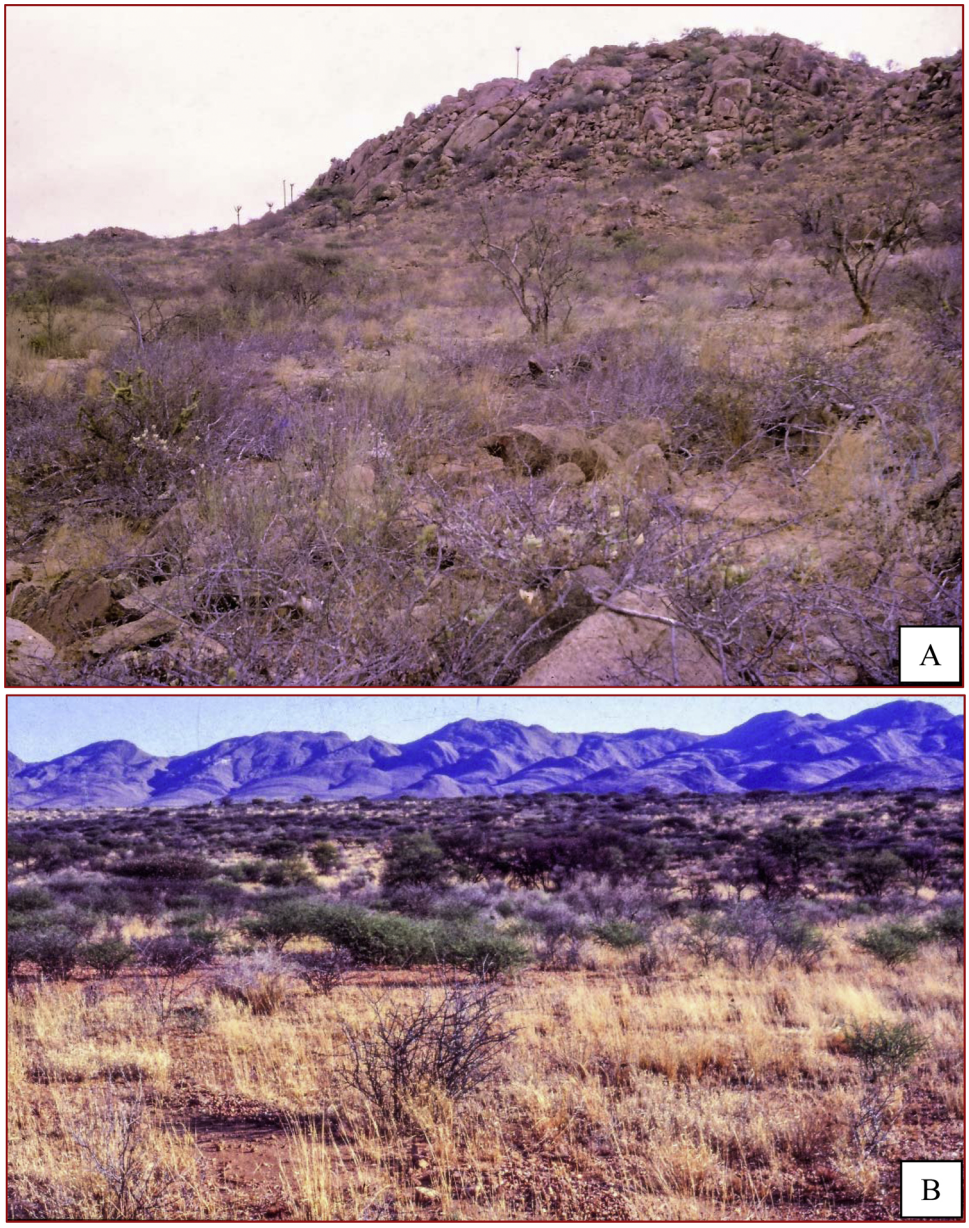

Fig. 15. Potential change in community structure in the Namib hot desert, Namibia from (A) present day desertic mainly shrub-grass *Commiphora dinteri, Enneapogon scaber* complex (Elevn. 1012 m, from 8.1 to predicted 11.8 °C Min. Temp. coldest month in year 2100), towards (B) more dominant shrubland *Boscia foetida, Enneapogon scaber, Stipagrostis* spp. (elevn. 520 m, present day Min. Temp. coldest month 11.8 °C). [Photographs by F. Venter].

which assemblages of PFTs and PFEs correspond to change in bioclimate both present and future and at varying scales. Ultimately, under future climate scenarios, the performance of plant based indicators of response to climate change will be judged mainly through their additional contribution at global scale to predictive vegetation models such as Dynamic Global Vegetation Models (DGVMs). This is supported by a global mapping of different FTs by Van Bodegom et al. (2011) who found that extreme global variability in FTs such as leaf mass per unit area, seed mass and specific stem density was not accounted for in current DGVMs. According to Yang et al. (2015) the integration of FTs into DGVMs will be a critical step, towards improving the results of simulations. Examples of FTs include specific leaf area (SLA), leaf nitrogen content (LNC), carbon isotope composition of leaves (Leaf $\delta^{13}C$), the ratio between leaf-internal and ambient mole fractions of CO_2 (leaf internal and leaf ambient Ci /Ca), seed mass and plant height, considered by Yang et al. (2015) to be the most important in constructing DGVMs as they are based on FTs which are also recognized as important ecological strategies for plants (see also Yang et al., 2018). The degree to which simulations based on such data may apply worldwide remains to be tested, especially in remote areas where vegetation is poorly known and laboratory access problematic. Improvements in remotely sensed linkages with plant performance such as leaf N, lignin %, leaf mass per unit area, carotenoids, chlorophyll, leaf Ca and P, non-structural carbohydrates as well as other elements of plant biochemistry (Asner and Martin, 2016; Jetz et al., 2016), may offer a useful bridge in linking the parameters described by Yang et al. (2015, 2018) including the modal PFTs described in this paper.

Covariation of leaf traits and its controls across climates and biomes by Yang et al. (2018) revealed four orthogonal dimensions of total trait variation in which photosynthetic capacities (maximum carboxylation rate *V*cmax, maximum electron transport rate *J*max at 25 °C), leaf area and internal-to-ambient CO_2 ratio co-varied with moisture index and where site, climate, life form and family together explained 70% of trait variance. These results tend to be consistent with findings in the present

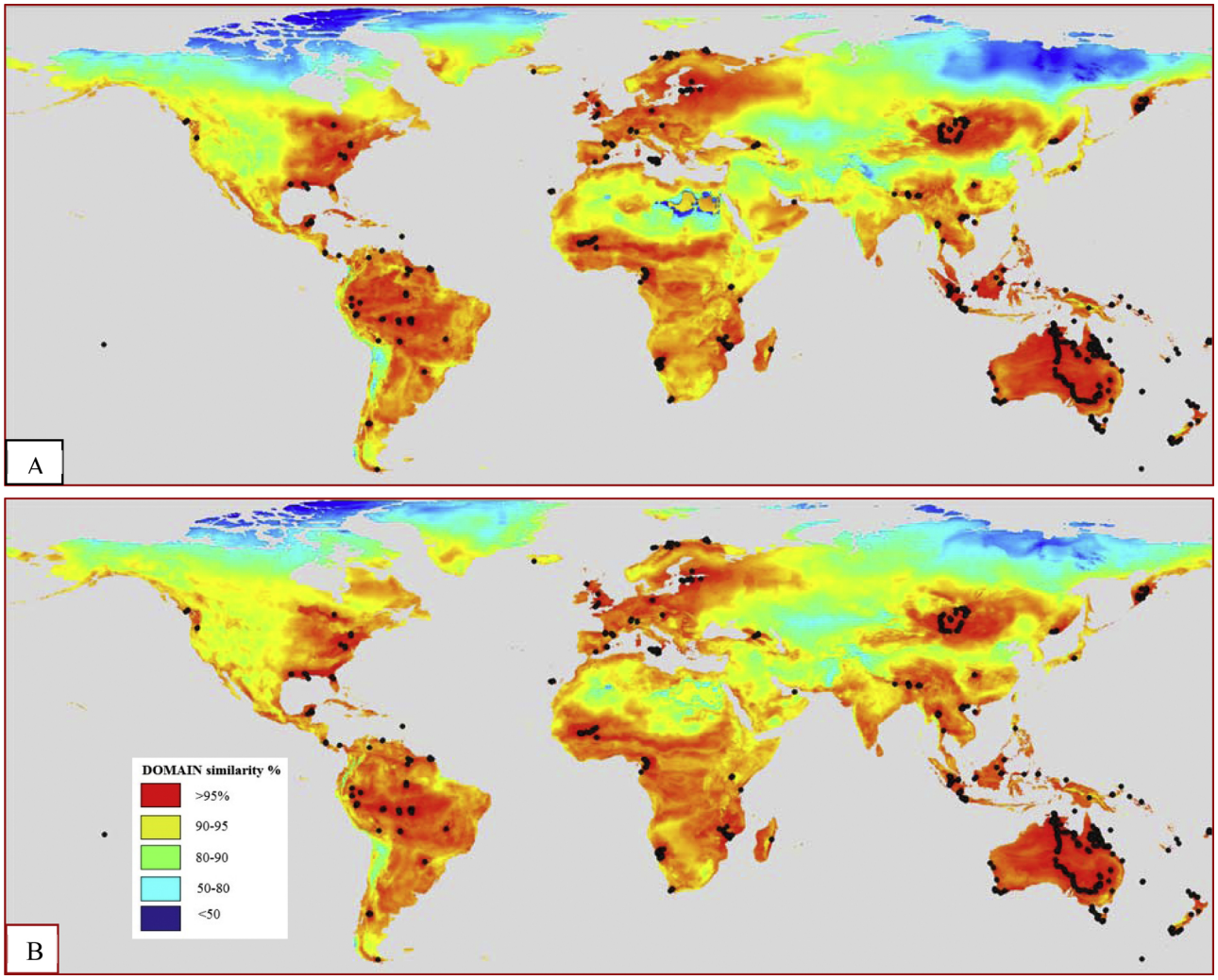

Fig. 16. Change in global bioclimate from (A) present day to (B) year 2100. Black dots indicate distribution of 1327 (40 m × 5 m) transect locations. Domain similarity model is based on ten bioclimate variables listed in Table 4. Trends show increased warming in high latitudes and elevation in (B). Legend insert shows approximate levels of climate similarity (red = 100%).

paper where specific modal PFTs and PFEs each co-varied with regional moisture availability but with differing correlates. These differences again question the level of functional information carried by both PFT and individual PFEs that can be used in predictive modeling (*cf.* Douma et al., 2012). This in turn also raises concerns about the predictive value of individual FTs used by Yang et al. (2018) and others (Kaplan, 2001, 2003; Allen et al., 2010; Smith, 2012; Hoogakker et al., 2016; Moncrieff et al., 2016; Valdes et al., 2017; Bloomfield et al., 2018; Madani et al., 2018). By linking three FTs (Specific Leaf Area (SLA), height, and seed mass) with local climate and primary productivity Madani et al. (2018) showed that future climate change (year 2070) might promote a shift in global plant traits resulting in changes in Gross Primary Productivity. While the models applied by Madani et al. (2018) provide a compelling argument for the use of such minimal sets of FTs, for the reasons outlined above, there are other well established FTs and modal PFTs including those in the present study that could complement such a study.

The correlative analyses between PFTs, PFEs and bioclimate show highly significant relationships under both present and future climate scenarios. Certain PFEs involved in these correlative patterns include functional traits rarely used in field surveys. Among these is leaf form defined by bifacial dorsiventral (do) (mostly hypostomatous) and isobilateral and isocentric (is) (isostomatous or amphistomatic) forms that play a vital role in the stomatal control of plant atmospheric fluxes and vascular hydraulics in climates past and present and, most likely, future (Roth-Nebelsick and Konrad, 2018, this volume). As indicated in the preceding paper (Gillison, this volume), leaf inclination – a feature readily observed in the field – using four basic classes, is a well established functional trait and, as shown in this paper, is highly correlated with bioclimate. Of equal or perhaps greater interest is the unexpected and highly significant correlation of green stem or cortical photosynthesis (ct) with bioclimate and as an indicator of specific vegetation assemblages. As used in the present system, cortical photosynthesis is recorded only for phanerophytes (ligneous or semi-ligneous plants >2 m tall) as almost all chamaephytes carry this trait and thus possess little discriminatory value in comparative studies of community dynamics. In Table 10, modal PFTs with the ct trait, dominate the world's flora, at least, as indicated by the present global dataset containing 3403 uniquely different modal PFTs. The dominance of this trait, especially in extreme arid seasonal environments and in early to mid-seral stages of many tropical forests, suggests that a much closer examination is needed to better define its potential role in plant survival and physiological maintenance under extreme conditions. Where leaf loss is a recurrent phenomenon (e.g. via freezing or drought, or both), cortical photosynthesis may compensate for reduced overall photosynthesis (A_{max}) and contribute to plant survival by re-fixing metabolic, internal stem carbon or, possible gas exchange via lenticillate stems. This trait is also particularly evident among ligneous and semi-ligneous, succulent CAM plants in arid extremes as in some hot deserts and semi-

Table 10
Percentage of modal PFTs and PFEs (PFT trait elements) occurring in the present day global flora.*

Modal PFT	Total	Percent	PFE	Total	Percent
me-la-do-ct-ph	1622	4.480	dorsiventral (do)	34334	18.647
no-la-do-ct-ph	1085	2.997	lateral incl (la)	18973	10.305
me-la-do-ph	925	2.555	phanerophyte (ph)	14701	7.984
no-la-do-ph	825	2.279	hemicryptophyte (hc)	11085	6.020
me-la-do-ch	824	2.276	vertical incl. (ve)	9360	5.084
no-la-do-ch	802	2.215	microphyll (mi)	9011	4.894
me-la-do-ph-li	613	1.693	mesophyll (me)	8738	4.746
mi-la-do-ch	602	1.663	notophyll (no)	8692	4.721
no-la-do-ph-li	596	1.646	chamaephyte (ch)	7883	4.281
mi-la-do-ct-ph	434	1.199	adventitious (ad)	7237	3.931
no-co-do-ph	393	1.085	cortical P/S (ct)	5951	3.232
na-ve-do-ch	374	1.033	lianoid (li)	5479	2.976
mi-ve-do-ch	373	1.030	parallel vein (pv)	5409	2.938
mi-la-do-ph	300	0.829	nanophyll (na)	5251	2.852
pl-la-do-ct-ph	297	0.820	deciduous (de)	5205	2.827
mi-la-do-ph-li	289	0.798	composite leaf incl. (co)	5130	2.786
mi-la-do-hc	272	0.751	pendulous incl. (pe)	2736	1.486
me-co-do-ph	270	0.746	rosulate (ro)	2437	1.324
na-ve-do-pv-hc	265	0.732	epiphyte (ep)	2230	1.211
na-ve-do-hc	255	0.704	succulent (su)	2230	1.211
Total counts	36207	100.000		184122	100.000

* Top 20 modal PFTs and PFEs (Plant functional elements) from worldwide total of 1327 (40 m × 5 m) transect plots with 36207 counts containing 3403 species-weighted, modal PFTs and 36 generic PFEs. Total species records 25637. Each plot recorded all vascular plant species and modal PFTs. See Table 1 for complete trait element codes.

arid seasonal zones, suggesting that a compensatory mechanism of this kind may be critical in ensuring plant survival under climate change especially under increasing seasonal extremes. In more mesic, less seasonal environments in the humid tropics, there is evidence that ct may be a facultative response in certain families (typically Cercropiaceae, Euphorbiaceae) to disturbance gaps in forest canopy and in successional sequences (Gillison et al., 2013).

Solidiform, (so) succulent (su) and rosette (ro) traits, while widespread globally, are especially characteristic of seasonally arid and desertic environments as typified by many succulent 'cactoid' and rosette 'bromelioid' plants, especially those with CAM metabolism (Williams et al., 2014; Ávila-Lovera et al., 2017). While the approximately 10,000 succulent taxa constitute less than 3 percent of the world's vascular plant species, they occupy very significant areas of the planet (*cf.* Oldfield, 1997). It is surprising therefore that global databases such as GLOPNET (Wright et al., 2004) and TRY (Kattge et al., 2011) contain remarkably few references to these wide-ranging and globally significant plant types, thus limiting their value as a global data resource in modeling future climate vegetation composition. One possibility for this lack of inclusion is that certain laboratory based measurements such as SLA are problematic among many succulents such as cacti. The present study has demonstrated that plants possessing these functional traits can be readily recorded in the field using the current methodology and successfully applied as indicators of plant response to climate as well as biodiversity (Gillison et al., 2013). Apart from individual PFTs and PFEs, a measure of plant functional complexity (PFC) also shows predictive linkages with bioclimate, notably in high latitude arctic-boreal conditions (Table 3) where it carries more predictive power than either species or PFT richness.

The plant–climate patterns identified in present day vegetation were used to identify likely changes in the year 2100 based on estimates of Bioclim values for the latter. In almost every case, the statistical inferences outlining common trends in PFT and PFE response to bioclimate under present day conditions, are repeated for year 2100 with only relatively minor variations. However, these patterns take on a new meaning when related to likely future changes on the same or similar physical site (Figs. 11–15) where, for example, forested sites previously dominated by Fagaceae (*Castanopsis, Lithocarpus*) in equatorial Sumatra and Java are likely to adopt a different trajectory under climate change towards forest composition with fewer Fagaceae and more families typical of lowland types (e.g. Dipterocarpaceae, Anacardiaceae, Lauraceae), that are characterized by PFTs with larger leaves, green stem photosynthesis and increased numbers of lianas, epiphytes, ferns and fern-like PFTs. Rather than indicators of specific vegetation outcomes under climate change, the pictorial examples represent hypothetical reference points along a temporal trend line in which certain modal PFTs are likely to move in a way that ultimately influences vegetation composition – as to what that composition is likely to be, will be influenced by other extrinsic factors besides climate. Much depends on the biotic and abiotic context of initial prevailing environmental conditions that, depending on how they are described, define the 'Starting point' for predictive ecology (Gillison and Liswanti, 2004; Kimball et al., 2016).

As indicated in Figs. 11–15, physiognomy and structure are also key elements in vegetation composition. While these were not part of this study of functional types, the data are available in the same global data set and could be used to supplement investigations of vegetation response to climate change.

The analyses described in this treatment reveal a wide range of significant relationships across the five regions. As a general approximation, more than 50 percent of the regressions between PFTs, PFEs and most Bioclim variables (but especially minimum temperature of the coldest week, annual precipitation and seasonal (CV) soil Moisture Index), are statistically significant (frequently $P < 0.001$). With significantly more samples for the global database, the number of statistically significant indicators increases although with decreased adjusted r^2 values, indicating that scaling issues are significant, in addition to the strength of prevailing environmental gradients. While one of the strengths of the present approach is the improved functional information about whole-plant fitness described in a modal PFT rather than by single PFEs, one weakness is that the frequently large number of modal PFTs that can occur in a sample plot may be represented by a relatively low number of counts per PFT thus limiting their use in statistical analysis. Improved statistical modeling that can better account for frequent non-linearity may reveal even more statistically significant relationships. The results presented here nonetheless provide statistical support for many PFTs and their individual functional traits as indicators of change along bioclimatic gradients. Their similar displacement pattern alone in the year 2100 however, does not by itself provide a ready means of assessing the value of plant functional types and traits as indicators of vegetation composition under climate change. Using actual differences in the mean values of MAP in both climate scenarios as illustrated in the foregoing, as a baseline for correlative analysis suggests that this may offer some advantage in identifying response indicators.

With climate warming, for example, plant composition (taxa and PFTs) and vegetation structure at one biophysical location are likely to shift geospatially along a temporal gradient according to the degree of climate change. Geospatial shifts of this kind are thus likely to lead to changes in substrate, niche availability and species and PFT composition together with consequences for adaptive acclimation and an increasing likelihood of non-indigenous invasive species. While carrying considerable predictive value, in the regions under study, even the strongest correlates must also be viewed within the actual field context in order to identify the nature of the environmental filters. In the E. Himalaya region for example, a 'deciduous' PFE may indicate response to both high elevation freezing or lowland drought, while in the Gobi desert, slope and environmental aspect are highly significant.

The real value of the correlative relationships between plant functional types and traits and bioclimate detected in this study are therefore likely to be better realized as parameters in process-based Earth System and other predictive vegetation models described in the foregoing. One of the main obstacles in parameterizing models that

ARTICLE IN PRESS

simulate response to environmental change lies in the availability of data that adequately quantify ecophysiological response. There are many circumstances where laboratory based measures such as SLA, LDMC, A_{max}, leaf N, will be difficult to acquire at the necessary scale of plant functional performance from plot to biome. This can be further confounded through inconsistencies in the way key attributes are recorded, stored and accessed in emerging global databases. It is here that the readily observable functional variables used in the construction of modal PFTs may complement such ecophysiological parameters. For example there is increasing evidence that certain functional plant features used in the present study such as leaf stomatal distribution (typically dorsiventral abaxial or isobilateral or isocentric leaves), leaf inclination, green stem photosynthesis and related metabolic pathway (CAM, C_3, C_4) can be regarded as ecophysiologically significant input variables for dynamic vegetation modeling purposes. Given that vegetation structure and species and PFT composition on current physical locations are very likely to vary with climate change, vegetation composition on an original site may be indicated using existing plant functional correlative data for plant–climate relationships that match the forecasted bioclimate for that site.

5. Conclusions

This paper has addressed the potential role of plant functional traits and their combination as modal Plant Functional Types (PFTs) as current and future indicators of vegetation response to climate change under two specific climate scenarios. Exploratory data analyses support the use of modal PFTs as response indicators but also reveal different indicator value by the PFTs and their individual functional traits (PFEs), with the former carrying higher levels of functional information as a predictor across multiple scales within and between regions. As most predictive models are parameterized by individual traits, these results provide a compelling argument for comparing the relative performance of both modal PFTs and PFEs in predictive models such as Earth System and Dynamic Global Vegetation Models. The component PFEs used in this treatment are specifically selected to reflect key ecophysiological elements concerned directly with resource acquisition and conservation. Because they are also specifically designed for rapid recording in the field, they avoid the need for laboratory support that may not be accessible in many parts of the globe where there is an urgent need for further data. The data in this study were documented using a uniform protocol worldwide thereby facilitating comparative analysis and may complement more detailed ecophysiological measurements of plant function in other emerging global databases. In addressing the hypotheses listed in the introduction, the data analyses demonstrated that 1) modal PFTs present a useful alternative to PFTs and individual traits commonly applied in the current modeling environment; 2) In the present study, modal PFTs were more efficient indicators of vegetation response to climate change than individual PFEs; 3) A careful selection of functional traits using uniform methods of recording and analysis such as those undertaken here may lead to more informed parameterization of models such as ESMs and DGVMs. Finally, it is necessary to emphasize that the functional indicators identified here are but one element of the highly complex array of other factors that influence vegetation response to environmental change such as land use, species acclimation, invasive species and population pressure.

Acknowledgements

The data recorded for this study were acquired in many countries over several decades during which I received extensive and invaluable support from a very large number of colleagues, technical staff and others too numerous to mention individually. However, I especially thank former colleagues in the Australian Commonwealth Scientific and Industrial Research Organization (CSIRO), the Center for International Forestry Research (CIFOR) in Bogor Indonesia, the World Wildlife Fund for Nature, The World Bank, the Botanical Garden-Institute, Vladivostok, Russian Far East, The Instutute of Botany MAS Ulaanbaatar, Mongolia, the Ministry of Agriculture, Bhutan, the Gobabeb Desert Research Station, Namibia, the Chinese Academy of Forestry, Beijing and fellow members of the International Association for Vegetation Science for their assistance in numerous field sites in the Baltic, Scandinavian, Mediterranean and North American locations. Their cameraderie and support, often under difficult circumstances, is most gratefully acknowledged. T.H. Booth kindly provided comments on the draft as did F. Venter who also supplied photographs for the Namibian vegetation. D. Kriticos kindly assisted in the provision of Bioclim data. Four anonymous referees provided very useful advice. I also acknowledge the valuable assistance and continuing guidance from the Editor-in-Chief of Flora, H. Heilmeier in the preparation of papers I and II.

References

Ackerly, D.D., 2004. Functional strategies of chaparral shrubs in relation to seasonal water deficit and disturbance. Ecol. Monogr. 74, 25–44.
Albert, C.H., Thuiller, W., Yoccoz, N.J., Douzet, R., Aubert, S., Lavorel, S., 2010. A multi-trait approach reveals the structure and the relative importance of intra- vs. inter-specific variability in plant traits. Funct. Ecol. 24, 1192–1201.
Allen, J.R.M., Hickler, T., Singarayer, J.S., Sykes, M.T., Valdes, P.J., Huntley, B., 2010. Last glacial vegetation of northern Eurasia. Quat. Sci. Rev. 29, 19–20.
Asner, G.P., Martin, R.E., 2016. Convergent elevation trends in canopy chemical traits of tropical forests. Glob. Change Biol. 22, 2216–2227.
Ávila-Lovera, E., Zerpa, A.J., Santiago, L.S., 2017. Stem photosynthesis and hydraulics are coordinated in desert plant species. New Phytol. 216, 1119–1129.
Bardgett, R.D., 2005. The Biology of Soil: A Community and Ecosystem Approach. Oxford University press, Oxford.
Belbin, L., 1992. PATN Pattern Analysis Package; Technical Reference. CSIRO, Division of Wildlife and Ecology, Canberra, Australia.
Bernhardt-Römermann, M., Gray, A., Vanbergen, A.J., Bergès, L., Bohner, A., Brooker, R.W., De Bruyn, L., De Cinti, B., Dirnböck, T., Grandin, U., Hester, A.J., Kanka, R., Klotz, S., Loucougaray, G., Lundin, L., Matteucci, G., Mészáros, I., Oláh, V., Preda, E., Prévosto, B., Pykälä, J., Schmidt, W., Taylor, M.E., Vadineanu, A., Waldmann, T., Stadler, J., 2011. Functional traits and local environment predict vegetation responses to disturbance: a pan-European multi-site experiment. J. Ecol. 99, 777–787.
Bimeda, S.B., 2018. An Eco-physiological Response-based Vegetation Zonation on the Western Slope of Mt. Isarog Natural Park, Philippines. Active Grant: National Geographic Society.
Bloemen, J., Vergeynst, L., Overlaet-Michiels, L., Steppe, K., 2016. How important is woody tissue photosynthesis in poplar during drought stress? Trees 30, 63–72.
Bloomfield, K.J., Cernusak, L.A., Eamus, D., Ellsworth, D.S., Prentice, I.C., Wright, I.J., Boer, M.M., Bradford, M.G., Cale, P., Cleverly, J., Egerton, J.J.G., Evans, B.J., Hayes, L.S., Hutchinson, M.F., Liddell, M.J., Macfarlane, C., Meyer, W.S., Prober, S.M., Togashi, H.F., Wardlaw, T., Zhu, L., Atkin, O.K., 2018. A continental-scale assessment of variability in leaf traits, within species, across sites and between seasons. Funct. Ecol. 32, 1492–1506.
Booth, T.H., Nix, H.A., Hutchinson, M.F., Busby, J.R., 1987. Grid Matching: a new method for homoclime analysis. Agric. For. Meteorol. 39, 241–255.
Booth, T.H., Nix, H.A., Busby, J.R., Hutchinson, M.F., 2014. BIOCLIM: the first species distribution modeling package, its early applications and relevance to most current MAXENT studies. Divers. Distrib. 20, 1–9.
Box, E.O., 1981. Macroclimate and Plant Forms: An Introduction to Predictive Modeling in Phytogeography. Dr W. Junk, The Hague.
Box, E.O., 1996. Plant functional types and climate at the global scale. J. Veg. Sci. 7, 309–320.
Brohman, R., Bryant, L. (Eds.), 2005. Existing Vegetation Classification and Mapping Technical Guide. Gen. Tech. Rep. WO–67. U.S. Department of Agriculture Forest Service, Ecosystem Management Coordination Staff, Washington, DC, pp. 305.
Busby, J.R., 1991. BIOCLIM – a bioclimate analysis and prediction system. In: Margules, C.R., Austin, M.P. (Eds.), Nature Conservation: Cost Effective Biological Surveys and Data Analysis. CSIRO, Melbourne, pp. 64–68.
Carmona, C.P., Rota, C., Azcárate, F.M., Peco, B., 2015. More for less: sampling strategies of plant functional traits across local environmental gradients. Funct. Ecol. 29, 579–588.
Carpenter, G., Gillison, A.N., Winter, J., 1993. DOMAIN, a flexible modeling procedure for mapping potential distributions of plants and animals. Biodivers. Conserv. 2, 667–680.
de Bello, F., Carmona, C.P., Lepš, J., Szava-Kovats, R., Pärtel, M., 2016. Functional diversity through the mean trait dissimilarity: resolving shortcomings with existing paradigms and algorithms. Oecologia 180, 933–940.
Diaz, S., Lavorel, S., De Bello, F., Quétier, F., Grigulis, K., Robson, T.M., 2007. Incorporating plant functional diversity effects in ecosystem service assessments. P. Natl. Acad. Sci. (PNAS) U. S. A. 104, 20684–20689.
Díaz, S., McIntyre, S., Lavorel, S., Pausas, J.G., 2002. Does hairiness matter in Harare? Resolving controversy in global comparisons of plant trait responses to ecosystem disturbance. New Phytol. 154, 1–14.

ARTICLE IN PRESS

Díaz, S., Kattge, J., Cornelissen, J.H.C., Wright, I.J., Lavorel, S., Dray, S., Reu, B., Kleyer, M., Wirth, C., Prentice, I.C., Garnier, E., Bönisch, G., Westoby, M., Poorter, H., Reich, P.B., Moles, A.T., Dickie, J., Gillison, A.N., Zanne, A.E., Chave, J., Wright, S.J., Sheremet'ev, S.N., Jactel, H., Baraloto, C., Cerabolini, B., Pierce, S., Shipley, B., Kirkup, D., Casanoves, F., Joswig, J.S., Günther, A., Falczuk, V., Rüger, N., Mahecha, M.D., Gorné, L.D., 2016. The global spectrum of plant form and function. Nature 529, 167–171.

Douma, J.C., Aerts, R., Witte, J.P.M., Bekker, R.M., Kunzmann, D., Metselaar, K., van Bodegom, P.M., 2012. A combination of functionally different plant traits provides a means to quantitatively predict a broad range of species assemblages in NW Europe. Ecography 35, 364–373.

Elith, J., Franklin, J., 2013. Species distribution modelling. In: Levin, S. (Ed.), Encyclopedia of Biodiversity, second edn. Academic Press, Waltham MA, pp. 692–705.

Falster, D.S., Westoby, M., 2003. Leaf size and angle vary widely across species, what consequences for light interception? New Phytol. 158, 509–525.

Ferrer-Paris, J.R., Sanchez-Mercado, A., Rodríguez, J.P., Rodríguez, G.A., 2013. Using limited data to detect changes in species distributions: insights from Amazon parrots in Venezuela. Biol. Conserv. 173, 133–143.

Fontana, S., Petchey, O.L., Pomati, F., 2016. Individual-level trait diversity concepts and indices to comprehensively describe community change in multidimensional trait space. Funct. Ecol. 30, 808–818.

Franklin, J., Potts, A.J., Fisher, E.C., Cowling, R.M., Marean, C.W., 2015. Paleodistribution modeling in archaeology and paleoanthropology. Quat. Sci. Rev. 110, 1–14.

Gibson, A.C., 1996. Photosynthetic stems of nonsucculent plants. Gibson, A.C.: Structure–Function Relations of Warm Desert Plants. Adaptations of Desert Organisms. Springer, Berlin, Heidelberg, pp. 91–116.

Gillison, A.N., 1981. Towards a functional vegetation classification. In: Gillison, A.N., Anderson, D.J. (Eds.), Vegetation Classification in Australia. Commonwealth Scientific and Industrial Research Organization and the Australian National University Press, Canberra, pp. 30–41.

Gillison, A.N., 2002. A generic, computer-assisted method for rapid vegetation classification and survey, tropical and temperate case studies. Conserv. Ecol. 6, 3 [online].

Gillison, A.N., 2012. Circumboreal gradients in plant species and functional types. Bot. Pacifica 1, 97–107.

Gillison, A.N., 2013. Plant functional types and traits at the community, ecosystem and world level. In: van der Maarel, E., Franklin, J. (Eds.), Vegetation Ecology, second edition. John Wiley & Sons, Ltd, Oxford, UK, pp. 347–386 Ch. 12.

Gillison, A.N., 2016. Vegetation functional types and traits at multiple scales. In: Box, E.O. (Ed.), Vegetation Structure and Function at Multiple Spatial, Temporal and Conceptual Scales. Geobotany Studies, pp. 53–97.

Gillison, A.N., 2018. Latitudinal variation in plant functional types. In: Greller, A., Fujiwara, K., Pedrotti, F. (Eds.), Geographical Changes in Vegetation and Plant Functional Types. Geobotany Studies. Springer, Cham, pp. 21–57.

Gillison, A.N., Brewer, K.R.W., 1985. The use of gradient directed transects or gradsects in natural resource surveys. J. Environ. Manage. 20, 103–127.

Gillison, A.N., Carpenter, G., 1997. A generic plant functional attribute set and grammar for dynamic vegetation description and analysis. Funct. Ecol. 11, 775–783.

Gillison, A.N., Liswanti, N., 2004. Assessing biodiversity at landscape level: the importance of environmental context. In: Tomich, T.P., van Noordwijk, M., Thomas, D.E. (Eds.), Environmental Services and Land Use Change: Bridging the Gap between Policy and Research in Southeast Asia, pp. 75–86 Agric. Ecosyst. Environ. 104.

Gillison, A.N., Bignell, D.E., Brewer, K.R.W., Fernandes, E.C.M., Jones, D.T., Sheil, D., May, P.H., Watt, A.D., Constantino, R., Couto, E.G., Hairiah, K., Jepson, P., Kartono, A.P., Maryanto, I., Neto, G.G., Neto, R.J.V., van Noordwijk, M., Silveira, E.A., Susilo, F.-X., Vosti, S.A., Nunes, P.C., 2013. Plant functional types and traits as biodiversity indicators for tropical forests: two biogeographically separated case studies including birds, mammals and termites. Biodivers. Conserv. 22, 1909–1930.

Gillison, A.N., Asner, G.P., Fernandes, E.C., Richey, J.E., Sousa, D.L., da Cruz, E., Mafalacusser, J., Banze, A., Izidine, S., Fonseca, A.Rda, Pacate, H., 2016. Assessing biodiversity in dynamic landscapes: a new method for integrating rapid ground survey and remote sensing. J. Environ. Manage. 177, 9–19.

Gregory, K.M., 1996. Are paleoclimate estimates biased by foliar physiognomic responses to in-creased atmospheric CO_2? Palaeogeogr. Palaeoclimatol. Palaeoecol. 124, 39–51.

Grime, J.P., 1977. Evidence for the existence of three primary strategies in plants and its relevance to ecological and evolutionary theory. Am. Nat. 111, 1169–1194.

Hillebrand, H., 2004. On the generality of the latitudinal diversity gradient. Am. Nat. 163, 192–211.

Hoogakker, B.A.A., Smith, R.S., Singarayer, J.S., Marchant, R., Prentice, I.C., Allen, J.R.M., Anderson, R.S., Bhagwat, S.A., Behling, H., Borisova, O., Bush, M., Correa-Metrio, A., de Vernal, A., Finch, J.M., Frechette, B., Lozano-Garcia, S., Gosling, W.D., Granoszewski, W., Grimm, E.C., Grüger, E., Hanselman, J., Harrison, S.P., Hill, T.R., Huntley, B., Jimenez-Moreno, G., Kershaw, P., Ledru, M.-P., Magri, D., McKenzie, M., Müller, U., Nakagawa, T., Novenko, E., Penny, D., Sadori, L., Scott, L., Stevenson, J., Valdes, P.J., Vandergoes, M., Velichko, A., Whitlock, C., Tzedakis, C., 2016. Terrestrial biosphere changes over the last 120 kyr. Clim. Past 12 51e73.

Humphreys, R.K., Puth, M.T., Neuhäuser, M., Ruxton, G.D., 2019. Underestimation of Pearson's product moment correlation statistic. Oecologia 189, 1–7.

IPCC, Climate Change, 2007. In: Solomon, S., Qin, D., Manning, M., Chen, Z., Marquis, M., Avery, K., Tignor, M., Miller, H. (Eds.), The Physical Science Basis. Contribution of Working Group I to the Fourth Assessment Report of the Intergovernmental Panel on Climate Change. Cambridge University Press.

Jetz, W., Cavender-Bares, J., Pavlick, R., Schimel, D., Davis, F.W., Asner, G.P., Guralnick, R., Kattge, J., Latimer, A.M., Moorcroft, P., Schaepman, M.E., Schildhauer, M.P., Schneider, F.D., Schrodt, F., Stahl, U., Ustin, S.L., 2016. Monitoring plant functional diversity from space. Nat. Plants 2, 16024.

Jones, D.T., Susilo, F.-X., Bignell, D.E., Hardiwinoto, S., Gillison, A.N., Eggleton, P., 2003. Termite assemblage collapse along a land-use intensification gradient in lowland central Sumatra, Indonesia. J. Appl. Ecol. 40, 380–391.

Kaplan, J.O., 2001. Geophysical Applications of Vegetation Modeling, Ph.D. Thesis. Lund Univ., Lund, Sweden.

Kaplan, J.O., Bigelow, N.H., Bartlein, P.J., Christensen, T.R., Cramer, W., Harrison, S.P., Matveyeva, N.V., McGuire, A.D., Murray, D.F., Prentice, I.C., Razzhivin, V.Y., Smith, B., Walker, D.A., Anderson, P.M., Andreev, A.A., Brubaker, L.B., Edwards, M.E., Lozhkin, A.V., 2003. Climate change and Arctic ecosystems. II. Modeling, palaeodata-model comparisons, and future projections. J. Geophys. Res. Atmos. 108D19, 8171.

Kattge, J., Díaz, S., Lavorel, S., Prentice, I.C., et al., 2011. TRY - a global database of plant traits (126 authors). Glob. Change Biol. 17, 2905–2935.

Keddy, P.A., 1992. Assembly and response rules: two goals for predictive community ecology. J. Veg. Sci. 3, 157–164.

Kimball, S., Funk, J.L., Spasojevic, M.J., Suding, K.N., Parker, S., Goulden, M., 2016. Can functional traits predict plant community response to global change? Ecosphere 7, e01602.

Kriticos, D.J., Webber, B.L., Leriche, A., Ota, N., Bathols, J., Macadam, I., Scott, J.K., 2012. CliMond: global high resolution historical and future scenario climate surfaces for bioclimatic modeling. Methods Ecol. Evol. 3, 53–64.

Kriticos, D.J., Jarošik, V., Ota, N., 2014. Extending the suite of bioclim variables: a proposed registry system and case study using principal components analysis. Methods Ecol. Evol. 5, 956–960.

Lapola, D.M., Oyama, M.D., Nobre, C.A., Sampaio, G., 2008. A new world natural vegetation map for global change studies. An. Acad. Bras. Ciênc. (Ann. Braz. Acad. Sci.) 80, 397–408.

Lavorel, S., McIntyre, S., Landsberg, J., Forbes, T.D.A., 1997. Plant functional classifications, from general groups to specific groups based on response to disturbance. Trends Ecol. Evol. 12, 474–478.

Lavorel, S., Touzard, B., Lebreton, J.-D., Clément, B., 1998. Identifying functional groups for response to disturbance in an abandoned pasture. Acta Oecol. 19, 227–240.

Lavorel, S., McIntyre, S., Grigulis, K., 1999. Plant response to disturbance in a Mediterranean grassland: how many functional groups? J. Veg. Sci. 10, 661–672.

Lavorel, S., Díaz, S., Cornelissen, J.H.C., Garnier, E., Harrison, S.P., McIntyre, S., Pausas, J.G., Pérez-Harguindeguy, N., Roumet, C., Urcelay, C., 2007. Plant functional types: are we getting any closer to the Holy Grail? In: Canadell, J.G., Pataki, D., Pitelka, L. (Eds.), Terrestrial Ecosystems in a Changing World. The IGBP Series. Springer-Verlag, Berlin Heidelberg, pp. 149–160 Chapter 13.

Liu, J., Gu, L., Yu, Y., Ju, G., Sun, Z., 2018. Stem photosynthesis of twig and its contribution to new organ development in cutting seedlings of *Salix matsudana* Koidz. Forests 9, 207.

Ludwig, J.A., Cornelius, J.M., 1987. Locating discontinuities along ecological gradients. Ecology 68, 448–450.

Madani, N., Kimball, J.S., Ballantyne, A.P., Affleck, D.L.R., van Bodegom, P.M., Reich, P.B., Kattge, J., Sala, A., Nazeri, M., Jones, M.O., Zhao, M., Running, S.W., 2018. Future global productivity will be affected by plant trait response to climate. Sci. Rep. 8, 2870.

Magurran, A.E., 1988. Ecological Diversity and Its Measurement. Croom Helm, Australia.

Marks, C.O., Lechowicz, M.J., 2006. Alternative designs and the evolution of functional diversity. Am. Nat. 167, 55–66.

Mason, N.W.H., Pipenbaher, N., Škornik, S., Kaligarič, M., 2012a. Does complementarity in leaf phenology and inclination promote co-existence in a species-rich meadow? Evidence from functional groups. J. Veg. Sci. 94, 94–100.

Mason, N.W.H., de Bello, F., Mouillot, D., Pavoine, S., Dray, S., 2012b. A guide for using functional diversity indices to reveal changes in assembly processes along ecological gradients. J. Veg. Sci. 24, 794–806.

Mittelbach, G.G., Schemske, D.W., Cornell, H.V., Allen, A.P., Brown, J.M., Bush, M.B., Harrison, S.P., Hurlbert, A.H., Knowlton, N., Lessios, H.A., McCain, C.M., McCune, A.R., McDade, L.A., McPeek, M.A., Near, T.J., Price, T.D., Ricklefs, R.E., Roy, K., Sax, D.F., Schluter, D., Sobel, J.M., Turelli, M., 2007. Evolution and the latitudinal diversity gradient: speciation, extinction and biogeography. Ecol. Lett. 10, 315–331.

Moncrieff, G.R., Bond, W.J., Higgins, S.I., 2016. Revising the biome concept for understanding and predicting global change impacts. J. Biogeogr. 43, 863–873.

Myneni, R.B., Asrar, G., Kanemasu, E.T., Lawlor, D.J., Impens, I., 1986. Canopy architecture, irradiance distribution in leaf surfaces and consequent photosynthetic efficiencies in heterogeneous plant canopies. Part I. Theoretical considerations. Agric. and For. Meteorol. 37, 189–204.

Nedoff, J., Ting, I., Lord, E., 1985. Structure and function of the green stem tissue in Ocotillo (*Fouquieria splendens*). Am. J. Bot. 72, 143–151.

Oldfield, S., 1997. Cactus and Succulent Plants – Status Survey and Conservation Action Plan (comp.). IUCN/SSC Cactus and Succulent Specialist Group. IUCN, Gland, Switzerland and Cambridge, UK.

Parker, V.T., Schile, L.M., Vasey, M.C., Callaway, J.C., 2011. Efficiency in assessment and monitoring methods: scaling down gradient-directed transects. Ecosphere 2, 1–11.

Pfanz, H., 1999. Photosynthetic performance of twigs and stems of trees with and without stress. Phyton (Horn, Austria) 39, 29–33.

Pierce, S., Negreiros, D., Cerabolini, B.E.L., Kattge, J., Díaz, S., Kleyer, M., Shipley, B., Wright, S.J., Soudzilovskaia, N.A., Onipchenko, V.G., van Bodegom, P.M., Frenette-Dussault, C., Weiher, E., Pinho, B.X., Cornelissen, J.H.C., Grime, J.P., Thompson, K., Hunt, R., Wilson, P.J., Buffa, G., Nyakunga, O.C., Reich, P.B., Caccianiga, M., Mangili, F., Ceriani, R.M., Luzzaro, A., Brusa, G., Siefert, A., Barbosa, N.P.U., Chapin, F.S., Cornwell, W.K., Fang, J., Fernandes, G.W., Garnier, E., Le Stradic, S., Peñuelas, J., Melo, F.P.L., Slaviero, A., Tabarelli, M., Tampucci, D., 2017. A global method for calculating plant CSR ecological strategies applied across biomes world-wide. Funct. Ecol. 31, 444–457.

ARTICLE IN PRESS

Pillar, V.D., 1999. On the identification of optimal plant functional types. J. Veg. Sci. 10, 631–640.
Pillar, V.D., Sosinski, E.E., 2003. An improved method for searching plant functional types by numerical analysis. J. Veg. Sci. 14, 323–332.
Posada, J.M., Lechowicz, M.J., Kitajima, K., 2009. Optimal photosynthetic use of light by tropical tree crowns achieved by adjustment of individual leaf angles and nitrogen content. Ann. Bot. 103, 795–805.
Roth-Nebelsick, A., Konrad, W., 2018. Fossil leaf traits as archives for the past — and lessons for the future? Flora (in press).
Schimper, A.F.W., 1903. In: Fisher, W.R., Groom, P., Balfour, I.B. (Eds.), Plant-Geography Upon a Physiological Basis. The Clarendon Press, Oxford Transl.
Schulze, E.-D., 1982. Plant life forms and their carbon, water and nutrient relations. In: Lange, O.L., Nobel, P.S., Osmond, C.B., Ziegler, H. (Eds.), Encyclopedia of Plant Physiology, New Series 12B, Physiological Plant Ecology II. Springer, Berlin, pp. 615–676.
Smith, R.S., 2012. The FAMOUS climate model (versions XFXWB and XFHCC), description update to version XDBUA. Geosci. Model Dev. 5, 269–276.
USA National Park Service (NPS), 2012. Gradsect and field sampling plan for Amistad National Recreation area. Biblio. Gov 136.
Valdes, P.J., Armstrong, E., Badger, M.P.S., Bradshaw, C.D., Bragg, F., Davies-Barnard, T., Day, J.J., Farnsworth, A., Hopcroft, P.O., Kennedy, A.T., Lord, N.S., Lunt, D.J., Marzocchi, A., Parry, L.M., Roberts, W.H.G., Stone, E.J., Tourte, G.J.L., Williams, J.H.T., 2017. The BRIDGE HadCM3 family of climate models, HadCM3@Bristol v1.0. Geosci. Model Dev. 1–42.
Van Bodegom, P.M., Douma, J.C., Witte, J.P.M., Ordoñez, J.C., Bartholomeus, R.P., Aerts, R., 2011. Going beyond limitations of plant functional types when predicting global ecosystem–atmosphere fluxes: exploring the merits of traits-based approaches. Global Ecol. Biogeogr. 21, 625–636.
Van Bodegom, P.M., Douma, J.C., Verheijen, L.M., 2014. A fully traits-based approach to modeling global vegetation distribution. Proc. Natl. Acad. Sci. U. S. A. 111, 13733–13738.
Vandewalle, M., Purschke, O., de Bello, F., Reitalu, T., Prentice, H.C., Lavorel, S., Johansson, L.J., Sykes, M.T., 2014. Functional responses of plant communities to management, landscape and historical factors in semi-natural grasslands. J. Veg. Sci. 25, 750–759.
Violle, C., Navas, M.-L., Vile, D., Kazakou, E., Fortunel, C., Hummel, I., Garnier, E., 2007. Let the concept of trait be functional!. Oikos 116, 882–892.
Wang, W., Li, Z., Su, H., 2007. Comparison of leaf angle distribution functions: effects on extinction coefficient and fraction of sunlit foliage. Agric. For. Meteorol. 143, 106–122.
Wessels, K.J., Van Jaarsveld, A.S., Grimbeek, J.D., Van der Linde, M.J., 1998. An evaluation of the gradsect biological survey method. Biodivers. Conserv. 7, 1093–1121.
Westoby, M., 1998. A leaf–height–seed LHS plant ecology strategy scheme. Plant Soil 199, 213–227.
Williams, D.G., Hultine, K.R., Dettman, D.L., 2014. Functional trade-offs in succulent stems predict responses to climate change in columnar cacti. J. Exp. Bot. 65, 3405–3413.
Withrow, A.P., 1932. Life forms and leaf size classes of certain plant communities of the Cincinnati region. Ecology 13, 12–35.
Wong, J.L.G., Thornber, K., Baker, N., 2001. Resource Assessment of Non-wood Forest Products: Experience and Biometric Principles. Non-wood Forest Products No. 13. FAO, Rome CD-ROM included. ISBN 92-5-104614-X.
Wright, I.J., Reich, P.B., Westoby, M., Ackerly, D.D., Baruch, Z., Bongers, F., Cavender-Bares, J., Chapin, F.S.I.I.I., Cornelissen, J.H.C., Diemer, M., Flexas, J., Garnier, E., Groom, P.K., Gulias, J., Hikosaka, K., Lamont, B.B., Lee, T., Lee, W., Lusk, C., Midgley, J.J., Navas, M.-L., Niinemets, Ü., Oleksyn, J., Osada, N., Poorter, H., Poot, P., Prior, L., Pyankov, V.I., Roumet, C., Thomas, S.C., Tjoelker, M.G., Veneklaas, E., Villar, R., 2004. The worldwide leaf economics spectrum. Nature 428, 821–827.
Wrubel, E., Parker, V.T., 2018. Local patterns of diversity in California northern coastal scrub. Ecol. Evol. 8, 7250–7260.
Yang, Y., Zhu, Q., Peng, C., Wang, H., Chen, H., 2015. From plant functional types to plant functional traits: A new paradigm in modelling global vegetation dynamics. Prog. Phys. Geog. 39, 514–535.
Yang, Y., Wang, H., Harrison, S.P., Prentice, I.C., Wright, I.J., Peng, C., Lin, G., 2018. Quantifying leaf-trait covariation and its controls across climates and biomes. New Phytol. 221, 155–168.
Yiotis, C., Psaras, G.K., Manetas, Y., 2008. Seasonal photosynthetic changes in the green-stemmed Mediterranean shrub *Calicotome villosa*: a comparison with leaves. Photosynthetica 46, 262–267.
Zhang, J.-T., Xiao, J., Li, L., 2015. Variation of plant functional diversity along a disturbance gradient in mountain meadows of the Donglingshan reserve, Beijing, China. Russ. J. Ecol. 46, 157–166.